

Active Cell Balancing Algorithms in Lithium-ion Battery

Master's thesis in science

BOWEN JIANG

DEPARTMENT OF ELECTRICAL ENGINEERING

MASTER OF SCIENCE THESIS REPORT

Active Cell Balancing Algorithms in Lithium-ion Battery

BOWEN JIANG

Department of Electrical Engineering
CHALMERS UNIVERSITY OF TECHNOLOGY
Gothenburg, Sweden, 2020

Active Cell Balancing Algorithms in Lithium-ion Battery
BOWEN JIANG

© BOWEN JIANG, 2020

Supervisors:

Björn Fager, AVL MTC Motortestcenter AB
Ranjithh Raj Ram Prakash, AVL MTC Motortestcenter AB
Xiaoliang Huang, Chalmers University of Technology

Examiner:

Yujing Liu, Chalmers University of Technology

Department of Electrical Engineering
Chalmers University of Technology
SE-412 96 Gothenburg
Sweden
Telephone: +46 (0)31-772 1000

Typeset in LATEX
Printed by [Chalmers Reproservice]
Gothenburg, Sweden 2020

Summary

Lithium-ion batteries have been widely used in new energy vehicles (NEV) as large energy storage systems (EES). Balancing among series-connected cells is necessary to avoid overcharging or over-discharging as well as improve the amount of usable energy. Different from passive balancing, active balancing redistributes charges among cells or control cell output powers, further improving battery efficiencies. This thesis paper starts with the modeling of full-electric powertrain systems. Simulation results show that the range of the reference vehicle is extended when using active balancing in the battery system, comparing to passive balancing or no balancing. Afterward, a cell model is built based on 2-RC equivalent circuit theories, and a complete battery model is built by connecting cell models and taking considering of driving cycle requested power. A comprehensive review of existing passive balancing and active balancing methods is then carried out, and a summary comparing different balancing strategies is also given. One passive balancing method and three active balancing methods are selected out for modeling and simulation. Results show that switched resistor balancing has the easiest control algorithms but has the most energy losses. Single capacitor balancing only uses one capacitor but has longer balancing time. Multi inductor balancing has a bigger balancing current and faster balancing speed. Buck boost converter balancing has more flexible control algorithms, but more electrical components are needed.

A new active balancing topology and its control algorithms are finally proposed in this thesis paper. One supercapacitor is used in the balancing circuit which replaces the highest state of charge (SOC) cell and is charged during the vehicle regeneration process. The supercapacitor also transfers energy to the lowest SOC cell after it is fully charged. This new balancing strategy can not only improve balancing efficiency due to fewer times of energy conversion but also reduce balancing time compared to the single capacitor balancing.

Keywords: Active Balancing, Lithium-ion Battery, Full-electric Powertrain, Battery Management System

Acknowledgment

The thesis work has been carried out at the Department of Electrical Engineering at Chalmers University of Technology, Gothenburg, Sweden, and AVL MTC Motortestcenter AB, Gothenburg, Sweden.

I would like to express my most sincere thanks to,

- my examiner Yujing Liu for his valuable insights and always patient guidance.
- my supervisor Ranjithh Prakash and Xiaoliang Huang for giving me continuous supports and having regular meetings throughout the whole thesis work.
- my manager Björn Fager for giving me this wonderful opportunity to have researches on such an interesting topic.
- special thanks to colleagues from AVL GmbH, Graz, Austria for providing me necessary experimental data for cell modeling.

Bowen Jiang
Gothenburg, Sweden, June 2020

Contents

1	Introduction	1
1.1	Problem Background	1
1.2	Thesis Purpose	2
1.3	Limitations	2
2	Powertrain Modeling	3
2.1	Longitudinal Vehicle Dynamics	3
2.2	Battery Configuration Design	4
2.3	Full-electric Powertrain Modeling	6
3	Battery Modeling	8
3.1	Battery Cell Modeling	8
3.2	Battery Module Modeling	9
3.3	Complete Battery Modeling	10
4	Passive Balancing	12
4.1	Passive Balancing Review	12
4.1.1	Fixed Resistor Balancing	12
4.1.2	Switched Resistor Balancing	12
4.2	Passive Balancing Modeling	13
5	Active Balancing	15
5.1	Capacitor Based Active Balancing Review	15
5.1.1	Switched-Capacitor Balancing	15
5.1.2	Double-Tiered Switched-Capacitor Balancing	16
5.1.3	Chain Structure Switched-Capacitor Balancing	16
5.1.4	Parallel Structure Switched-Capacitor Balancing	16
5.1.5	Series-Parallel Structure Switched-Capacitor Balancing	17
5.1.6	Delta Structure Switched-Capacitor Balancing	18
5.1.7	Mesh Structure Switched-Capacitor Balancing	19
5.1.8	Chain Structure Double-Tiered Switched-Capacitor Balancing	19
5.1.9	Modularized Switched-Capacitor Balancing	19
5.1.10	Modularized Double-Tiered Switched-Capacitor Balancing	20
5.1.11	Single Switched-Capacitor Balancing	21
5.2	Inductor Based Active Balancing Review	22
5.2.1	Multi Inductor Balancing	22
5.2.2	Chain Structure Multi Inductor Balancing	22
5.2.3	Multi Tiered Inductor Balancing	23
5.2.4	Single Inductor Balancing	24
5.3	Converter Based Active Balancing Review	25
5.3.1	Boost Converter Balancing	25
5.3.2	Buck Boost Converter Balancing	26
5.3.3	Single Converter Balancing	26
5.3.4	Cuk Converter Balancing	26
5.3.5	Quasi Resonant Converter Balancing	27

5.3.6	Single Flyback Converter Balancing	28
5.3.7	Multi Flyback Converter Balancing	29
5.3.8	Multi Winding Flyback Converter Balancing	29
5.4	Active Balancing Modeling	31
5.4.1	Single Switched-Capacitor Balancing Modeling	31
5.4.2	Multi Inductor Balancing Modeling	32
5.4.3	Buck Boost Converter Balancing Modeling	34
6	New Proposed Active Balancing	36
6.1	Balancing Circuit	36
6.2	Balancing Algorithms	37
6.3	Balancing time calculation	38
7	Results and Analysis	39
7.1	Powertrain Simulation Results	39
7.2	Passive Balancing Simulation Results	41
7.3	Active Balancing Simulation Results	43
7.3.1	Single Switched-Capacitor Balancing Simulation Results	43
7.3.2	Multi Inductor Balancing Simulation Results	44
7.3.3	Buck Boost Converter Balancing Simulation Results	45
7.4	New Proposed Active Balancing Simulation Results	46
8	Conclusions	49
8.1	Conclusions	49
8.2	Future Work	49

1 Introduction

In order to meet requirements of high-efficiency and low-emission for future transportation, plug-in hybrid electric vehicles (PHEV) and battery electric vehicles (BEV) are considered to be the most viable choices, inside which energy storage systems (ESS) play key roles [1]. Compared to lead-acid batteries and NIMH batteries, lithium-ion batteries have many advantages, such as high energy densities, long cycle lives, low self-discharge rates, no memory effect, etc., which makes them more and more popular in recent decades, especially in automotive applications [2]. The nominal voltage of one single lithium-ion cell is around four volts, which is not possible to drive any PHEV or BEV powertrains. To solve this problem, hundreds or even thousands of cells are connected in series or parallel to construct battery modules and packs, so as to meet voltage and power requirements, as well as make vehicles have long enough driving ranges [3]. However, this series connection brings a tricky issue which is the cell-to-cell state of charge (SOC) unbalancing (shown in Figure 1.1), although the same type of cells are used in one battery. This unbalance phenomenon is mainly caused by two reasons. Firstly, cell manufacturing errors cause cell impedance values, open circle voltages (OCV), self-discharge rates, and aging rates to be different [4]. Secondly, uneven thermal management inside batteries makes cells be operated under different environments, which also has an influence on cell SOC [5]. As a result, cells with high SOC are fully charged before the others, and cells with low SOC tend to be fully discharged faster, which may make some cells over-charged or over-discharged under some situations and cause various abnormal phenomena, such as fast-aging, Li-plating, electrode structure disordering, even short-circuits and fires [6][7]. For the above reasons, battery management systems (BMS) with external balancing circuits are always necessary for batteries.

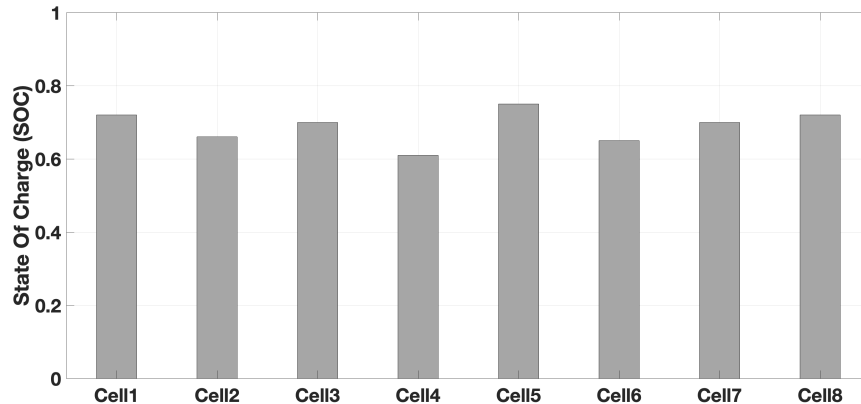


Figure 1.1: Unbalance of cell SOC

1.1 Problem Background

Battery balancing can be divided into two big categories: active balancing and passive balancing based on whether exceeded energy dissipation is in the form of heat [8]. Existing battery balancing methods have been categorized in Figure 1.2 based on literature reviews. Passive balancing is implemented by parallel connecting shunt resistors to high SOC cells, which is the most common balancing method used nowadays due to its low costs, small size, and easy control algorithms. However, the biggest disadvantages of passive balancing are low efficiency and additional burden to battery thermal management systems [9][8]. In contrast, active balancing is possible to redistribute charges among cells, improving powertrain system overall efficiency. Because of different utilized components, active balancing can be divided into three main groups: capacitor based, inductor based, and converter based [10][11]. But active balancing needs at least two times of energy conversion to transfer energy from high SOC cells to low SOC cells via energy storage components, which still brings much energy losses. However, if there is no balancing process in battery systems, both charging and discharging processes will be limited by one or several cells, reducing amounts of usable energy and vehicle ranges. Therefore, it is valuable to do some research on different passive and active balancing strategies and effects of battery balancing in vehicle powertrain systems.

1.2 Thesis Purpose

The objective of this thesis work is to study and compare different existing passive and active battery balancing typologies and their control algorithms, propose a new active balancing strategy, as well as integrate battery systems and powertrain systems together and improve overall performance in a real vehicle application. Powertrain models, passive balancing battery models, and active balancing battery models will be built with Simulink. A new active balancing strategy will be proposed which uses regeneration power to charge a supercapacitor, improving balancing speed and balancing efficiency of a reference vehicle. The improvement of the reference vehicle powertrain system due to passive or active balancing will also be studied and compared while taking consideration of driving cycle requirements.

1.3 Limitations

This thesis work is mainly focusing on battery and full-electric powertrain overall performance, so detailed characteristics of electric machines, motor inverters, and gear-boxes will not be studied. A simple vehicle model will be used by only considering longitudinal vehicle dynamics. Instead of electrochemical models, equivalent circuit models will be used for lithium-ion cell modeling, so cell aging process will not be simulated or studied. A simple heat convection model will be used for battery cooling system modeling, which assumes each cell is a thermal node and has heat transfer with constant temperature coolant.

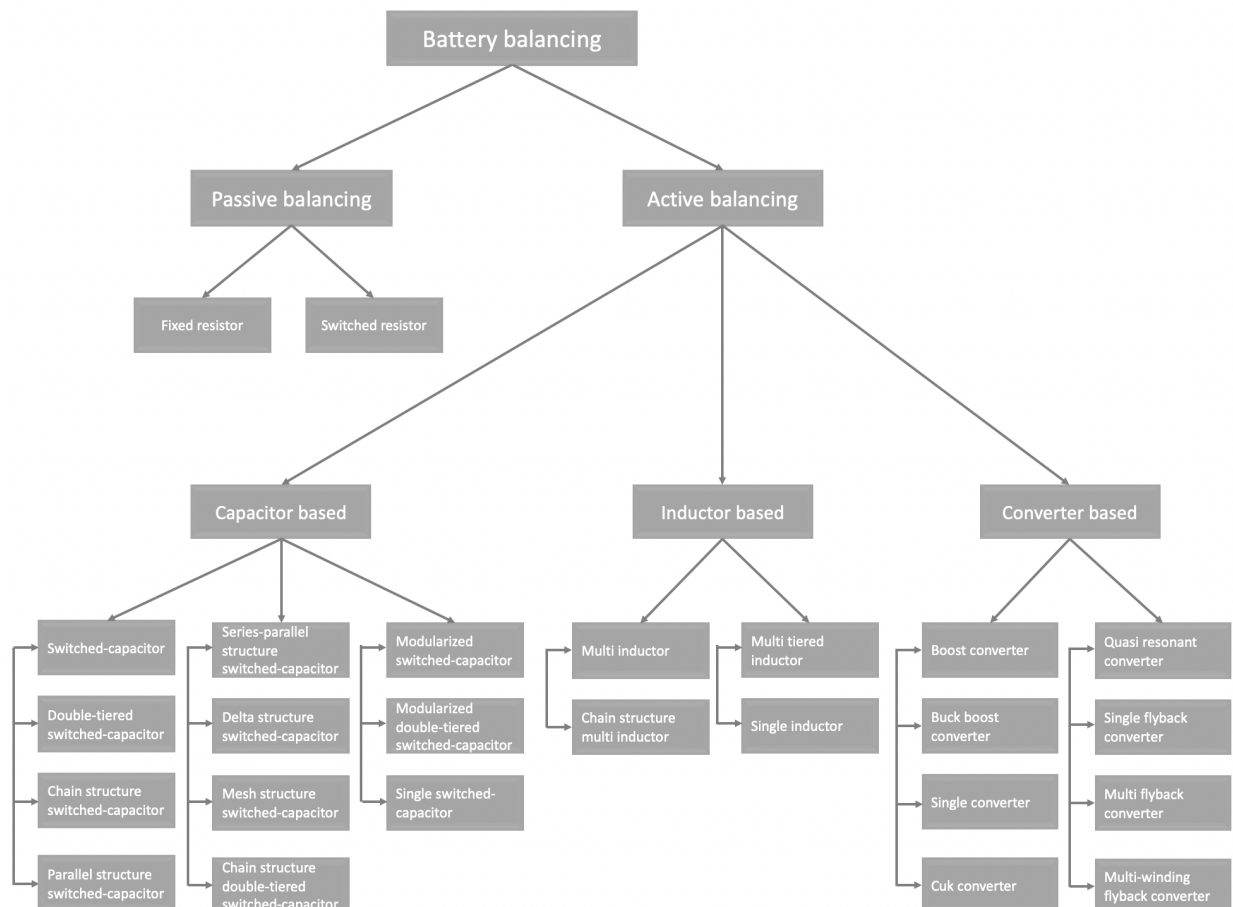


Figure 1.2: Tree diagram of battery balancing methods

2 Powertrain Modeling

Inside a full-electric powertrain, a battery system provides traction power to an electric motor, which can generate traction force to overcome vehicle air-drag force, rolling-resistance force, gradient force, and acceleration force. The Battery system shall be designed accordingly to meet vehicle energy and power requirements.

2.1 Longitudinal Vehicle Dynamics

As can be seen in Figure 2.1, a vehicle longitudinal free body diagram (FBD) is given. F_{trac} is traction force given by the powertrain system. F_{roll} is rolling resistance force on tires. F_{aero} is air-drag force. F_{grad} is gradient force due to gravity.

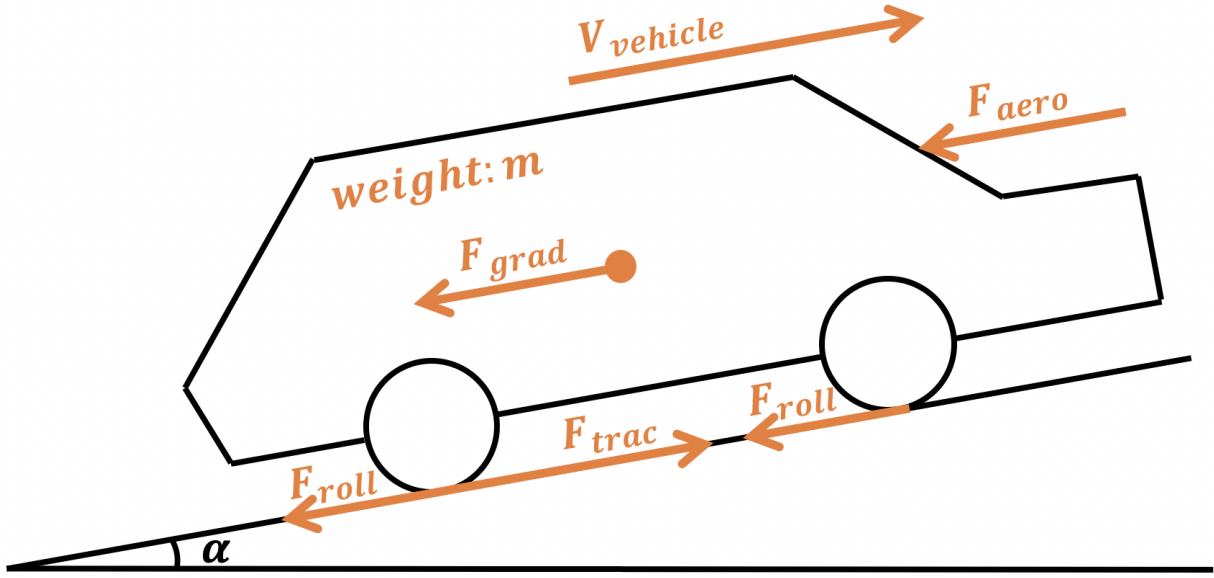


Figure 2.1: Longitudinal vehicle free body diagram

If vehicle speed ($V_{vehicle}$) direction is defined to be the positive direction, vehicle acceleration ($dV_{vehicle}/dt$) and requested vehicle power (P_{trac}) can be calculated in 2.1 and 2.2 [12]. Air-drag force is calculated from the air density (ρ), vehicle frontal area (A_f), air-drag coefficient (c_d), and vehicle relative speed to surrounding air ($V_{relative}$), which is shown in 2.3 [13]. Rolling resistance force is defined as longitudinal force losses on vehicle body compared to the longitudinal force which would have been transferred with ideal wheels, and is calculated from the rolling resistance factor (c_r) and vehicle mass (m). When the vehicle is driven on a slope it will also experience gradient force because of the gravity, which is related to the vehicle mass (m) and road angle (α) as calculated in 2.5 [12].

$$m \frac{dV_{vehicle}}{dt} = F_{trac} - (F_{aero} + F_{roll} + F_{grad}) \quad (2.1)$$

$$P_{trac} = F_{trac} V_{vehicle} \quad (2.2)$$

$$F_{aero} = \frac{1}{2} \rho A_f c_d V_{relative}^2 \quad (2.3)$$

$$F_{roll} = m g c_r \quad (2.4)$$

$$F_{grad} = m g \sin(\alpha) \quad (2.5)$$

Tesla Model 3 is one typical middle-size BEV. The standard-range version is selected as the reference vehicle for this thesis work. The reference vehicle parameters are according to [14] and some reasonable assumptions, which are listed in Table 2.1.

Table 2.1: Parameters of the reference vehicle

Reference vehicle parameters	Values
Mass	1611 kg
Frontal area	2.34 m ²
Air-drag coefficient	0.24
Rolling resistance coefficient	0.01
Wheel type	235/45 R18
Maximum motor power	211 kW
Battery capacity	50 kWh
Battery nominal voltage	350 V
Maximum speed	209 km/h
Acceleration 0-100 km/h	5.6 s
Full electric range	429 km

"Worldwide Harmonized Light-duty Vehicle Test Cycles (WLTC)" is used as the driving cycle in this thesis work, which consists of four stages: low speed, medium speed, high speed, and extra high speed [15]. Acceleration, braking, stopping, and other vehicle operation modes are included and shown in Figure 2.2.

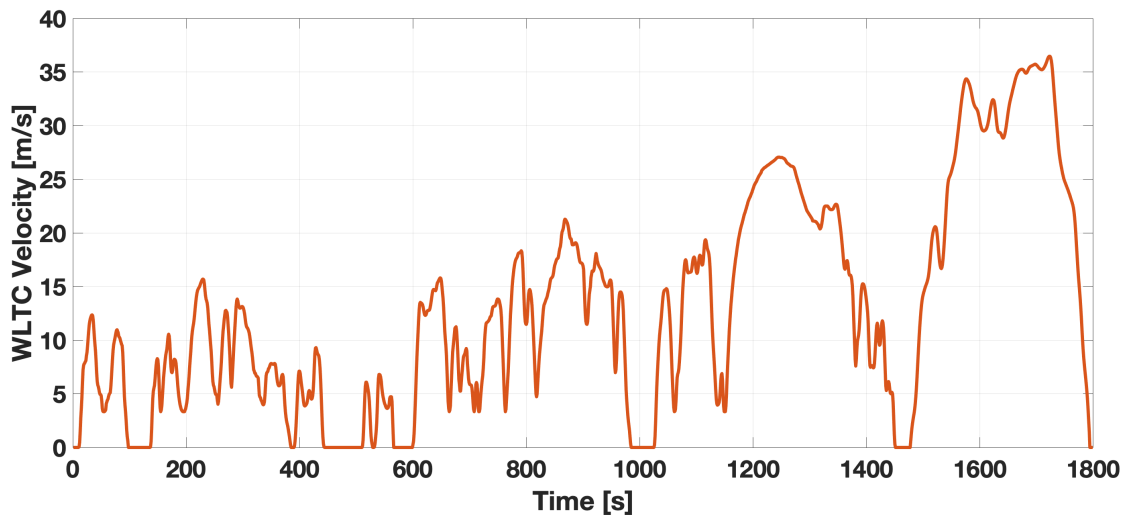


Figure 2.2: WLTC driving circle

2.2 Battery Configuration Design

24Ah lithium-ion pouch cells are used in this thesis work, whose experimental data are from the industry supervisor company. Some parameters of the cell are listed in Table 2.2. Cell energy capacity, which is about 90 Wh, can be calculated by integrating its OCV data. Since the battery of the reference vehicle has a capacity of 50 kWh and a nominal voltage of 350 V, the total cell number (N_{cell}) and series-connected cell number (N_{series}) are calculated in Equation 2.6 and Equation 2.7 to meet these requirements.

$$N_{cell} = \frac{50 \text{ kWh}}{90 \text{ Wh}} \approx 556 \quad (2.6)$$

$$N_{series} = \frac{350 \text{ V}}{3.7 \text{ V}} \approx 95 \quad (2.7)$$

Table 2.2: Parameters of the 24Ah lithium-ion pouch cell

Cell parameters	Description or values
Cell nominal capacity	24 Ah
Cell nominal voltage	3.7 V
Cell operating voltage range	2.5 V-4.2 V
Cathode material	LMO
Anode material	Graphite

As calculated above, at least ninety-five cells need to be connected in series to meet the battery nominal voltage requirement. But it is very hard to have a battery module with ninety-five series-connected cells inside. Firstly, the module size will be too big and could bring some packing problems. Secondly, much more balancing components will be used with an increasing number of series-connected cells in one module, which will also reduce balancing speed and balancing efficiency as well as make balancing algorithms more complex. For the above reasons, eight cells are connected in series to build a battery module, and twelve battery modules are connected in series to build a battery pack. To meet the requirements of battery capacity and power, six battery packs are connected in parallel to get a complete battery (Figure 2.3).

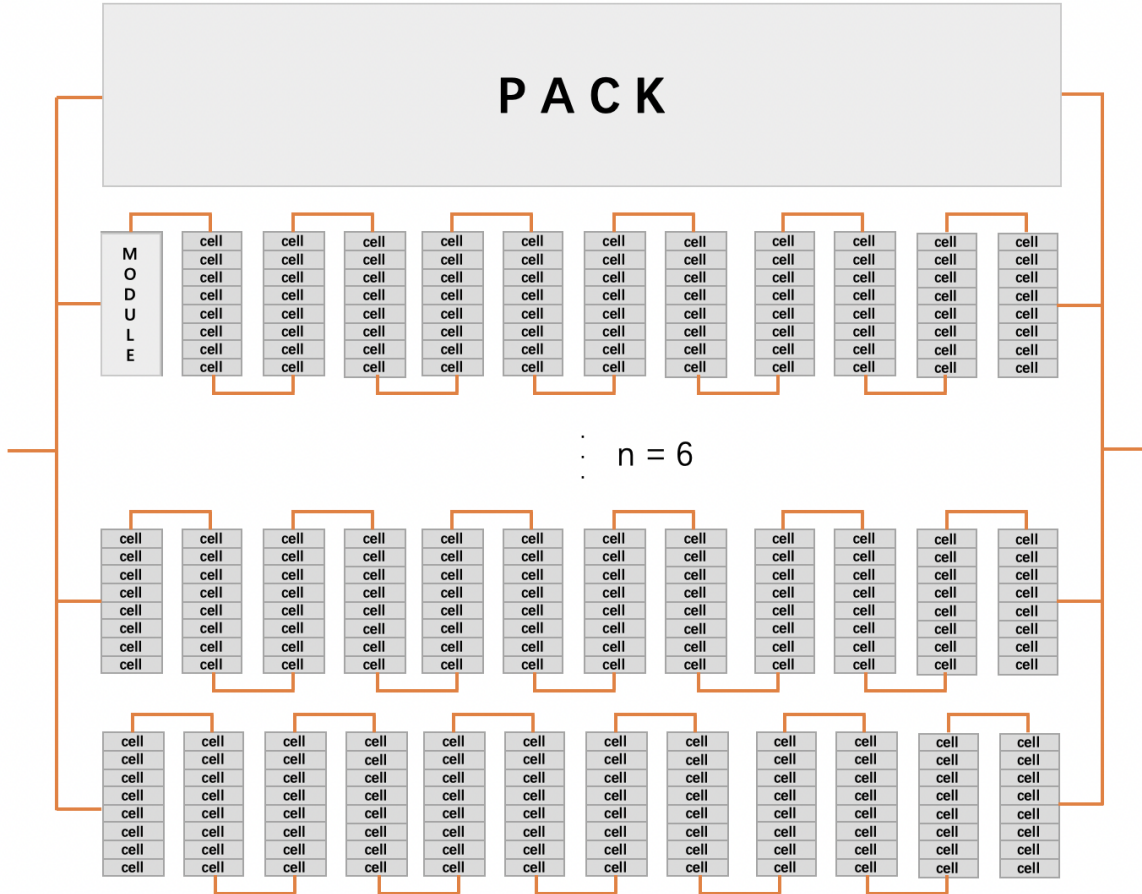


Figure 2.3: Proposed battery configuration

If the cell maximum discharging rate is 4C, the maximum power ($P_{maximum}$) of the above battery configuration is calculated in Equation 2.8, which also meets the reference vehicle requirement.

$$P_{maximum} = (3.7\text{ V} \times 96) \times (24\text{ Ah} \times 4\text{ C}) \times 6 = 205\text{ kW} \quad (2.8)$$

2.3 Full-electric Powertrain Modeling

QSS toolbox is a simulation tool for the design and optimization of powertrain systems, which is developed in the Simulink environment by Swiss Federal Institute of Technology in Zurich (ETH Zurich) [16][17]. Because of its high flexibility and extremely short calculation time, this toolbox is used for full-electric powertrain modeling in this thesis work.

As can be seen in Figure 2.4, a full-electric powertrain model is built. Different powertrain components are represented by different QSS toolbox blocks. Vehicle acceleration is calculated in the driving circle block, which together with vehicle speed works as inputs to the vehicle block. Inside the vehicle block, longitudinal vehicle dynamics explained in 2.1 are used for calculating vehicle traction force. In the wheel block, vehicle speed, acceleration, and traction force are transformed into rolling speed, rolling acceleration, and torque on wheels by using wheel parameters. In the gear-box block, a constant gear transmission efficiency is used. Since speed and torque ranges of electric motors are much larger compared to internal combustion engines, only one pair of gears is used in the gear-box block. Electric motor operating points are determined in the electric machine block by using speed and torque information from the gear-box block. As explained before, there is a total of seventy-two battery modules in a complete battery. But unbalance among the modules is ignored in this thesis work, and the battery is scaled down to have only one module (eight cells). Powertrain requested power is given out from the electric machine block after considering electric motor efficiency, which is also scaled down and sent to eight cell blocks.

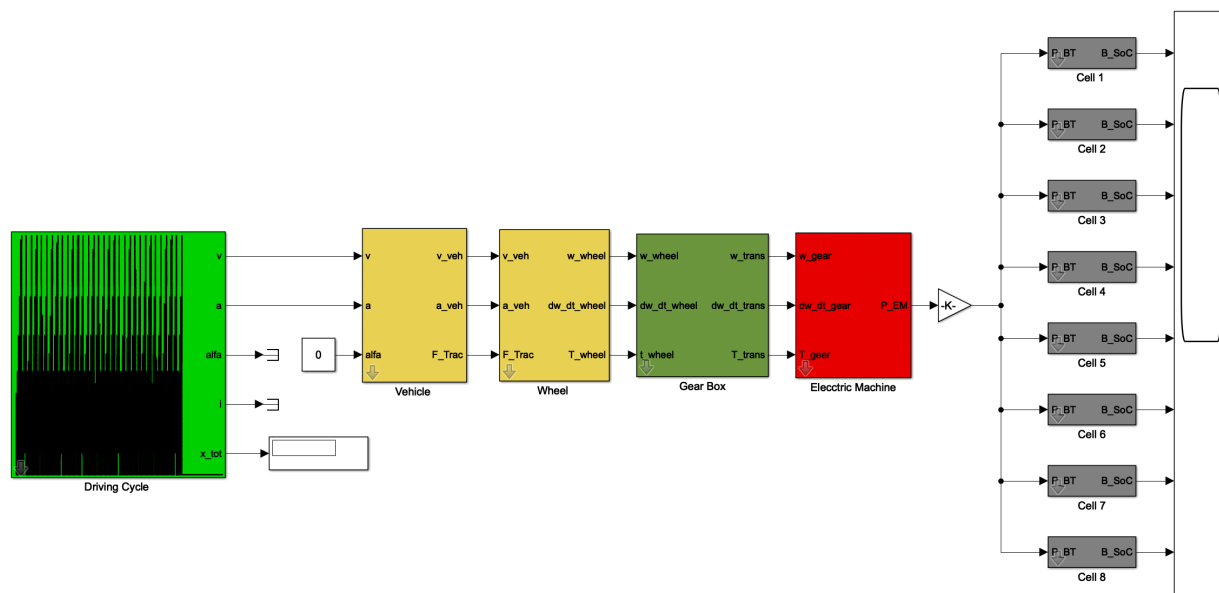


Figure 2.4: Full-electric powertrain, without balancing and with passive balancing

When there is no balancing, the full-electric powertrain model is shown in Figure 2.4. Since there is no balancing process, all cells always have the same charging power and the charging process will be stopped when the SOC of one cell reaches 1, which means not all cells can be fully charged. Therefore, SOC of eight cells are different at the beginning of the discharging process. What's more, because of manufacturing errors and various aging states, different cells also have different capacities. Initial SOC values and capacities are set in the eight cell blocks.

When there is passive balancing, the full-electric powertrain model is the same as shown in Figure 2.4. The only difference is the setting of initial SOC values. Because of the passive balancing, the battery charging process will not be stopped until SOC of all cells reach their upper limits. For this reason, initial SOC values of all cells are set to 1 before the discharging process starts.

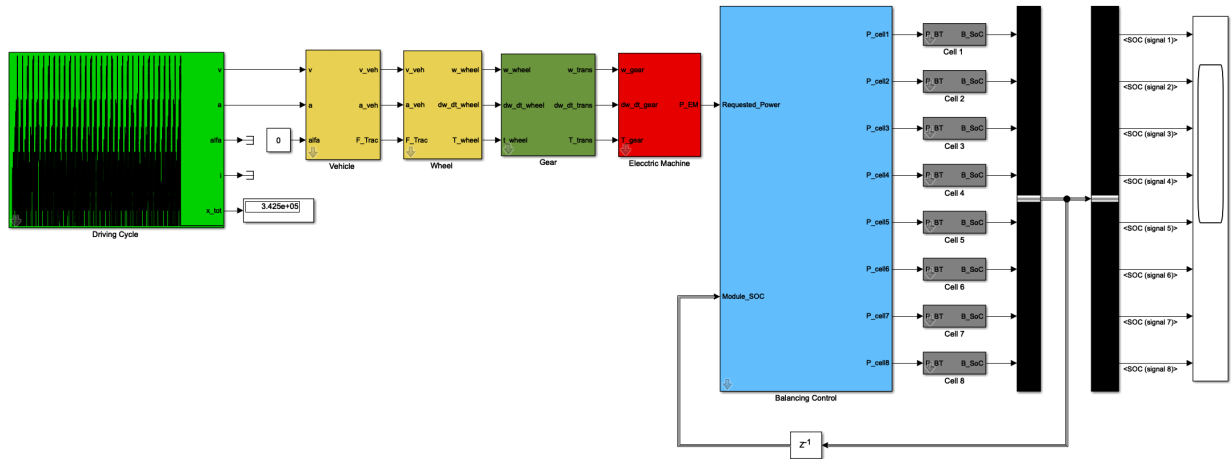


Figure 2.5: Full-electric powertrain, with active balancing

When there is active balancing, the full-electric powertrain model is shown in Figure 2.5. There is a balancing control block, where active balancing algorithms are included (Figure 2.6). Firstly, all cells can be fully charged because of controlled charging power to each cell. Initial SOC values of all cells are set to 1. Different from the passive balancing, SOC values of all cells are kept being monitored during the discharging process. If the difference between the maximum SOC and minimum SOC is bigger than a threshold value, the active balancing will be activated. The cells with higher SOC will be discharged faster. And less power is drawn from the lower SOC cells. The active balancing process will be stopped when the SOC difference is smaller than that threshold value. By using active balancing, all cells are fully discharged at the same time.

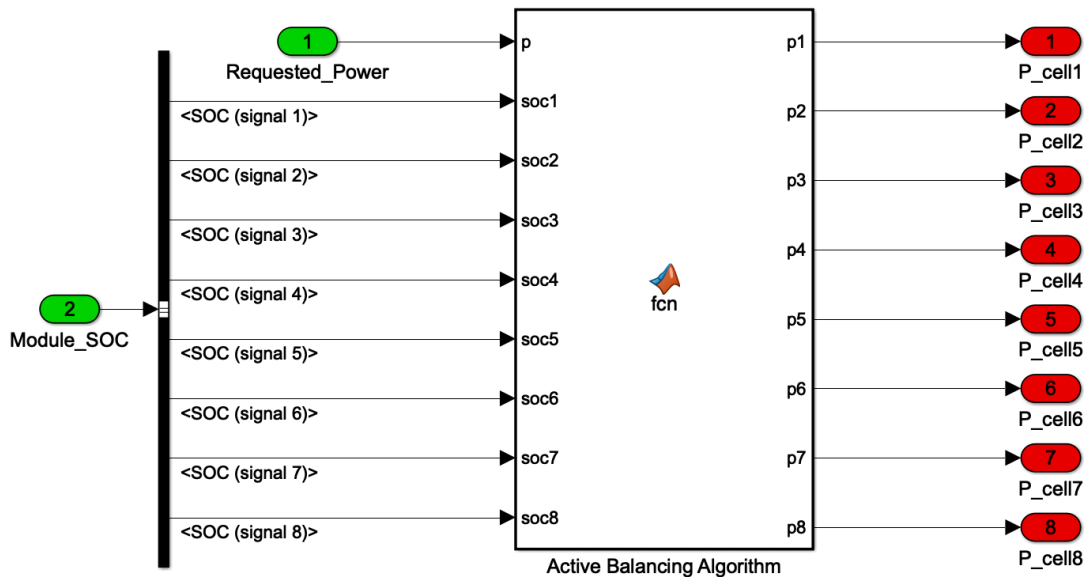


Figure 2.6: Full-electric powertrain with active balancing, balancing control block

In conclusion, batteries without balancing can't be fully charged and fully discharged, which have the smallest amounts of usable energy. Batteries with active balancing can be fully charged and discharged, which can utilize all usable energy. Battery with passive balancing can be fully charged but can't be fully discharged, whose usable energy amounts are between the other two designs.

3 Battery Modeling

A battery model is introduced in this section. As explained, the balancing process is applied in one battery module (among eight cells) in this thesis work. Therefore, the battery model is also scaled down and has only one battery module, balancing electrical circuits, and balancing algorithms. This battery model works as a platform and different passive and active balancing methods will be integrated with it in subsection 4.2 and subsection 5.4 for balancing performance studies.

3.1 Battery Cell Modeling

One Lithium-ion cell is mainly composed of positive and negative electrodes, electrolyte, one separator, and two current collectors. Movement of electrons and lithium-ions makes the transformation of electric energy and chemical energy possible [18]. There are three types of lithium-ion cell models: electrochemical models, empirical models, and equivalent circuit models [19]. Electrochemical models are very powerful to describe cell internal chemical reactions and the aging process by using differential equations. But calculation costs are quite high in electrochemical models. Empirical models describe characteristics of cells by multiple formulas, but they are normally less accurate. Equivalent circuit models use electrical circuits to simulate cell performance. The simplest one is to use one constant voltage source series connected with an internal resistor, but this model is less effective to analyze any cell dynamic performance. For this reason, 2-RC or 3-RC equivalent circuit models are introduced in some paper, which are very useful in SOC or SOH estimation and widely used in advanced BMS [20].

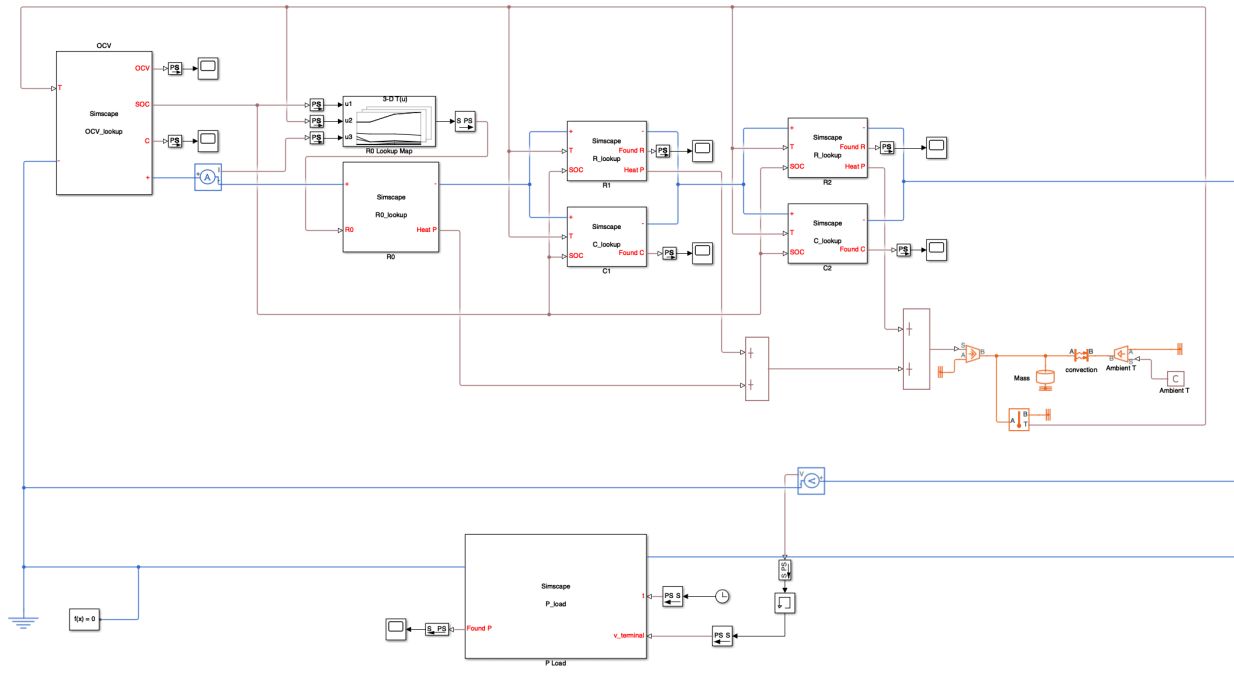


Figure 3.1: 2-RC equivalent circuit cell model

The 2-RC equivalent circuit model is used for lithium-ion cell modeling here, which is shown in Figure 3.1. Customized Simscape blocks are used to construct the equivalent circuit. The OCV Simscape block represents the open circuit voltage whose value changes with cell SOC and temperature, and cell SOC is also calculated in this block by using the method of Coulomb integration. The R0 Simscape block represents the internal resistance of electrodes, electrolytes, separators, and current collectors. The R0 value changes with cell SOC, temperature, and current passing through it, so a 3D lookup map is utilized and a current sensor is connected in the circuit as well. The R1 and C1 Simscape blocks are the first RC couple, which represents

the charge transfer process happening in negative and positive electrodes. The R2 and C2 Simscape blocks are the second RC couple and represent the lithium-ion diffusion process happening inside and outside active electrode material. The values of R1, C1, R2, C2 also change with cell SOC and temperature [18][21].

In order to get the cell temperature, cell internal heat needs to be calculated. According to [5], cell internal heat consists of irreversible heat and reversible heat. The irreversible heat is also called Joule heat, which is caused by currents passing through cell internal resistance. The reversible heat is caused by chemical reactions in both electrodes. In this thesis work, only irreversible heat is considered, and the heat of R0, R1, and R2 are calculated in their own Simscape blocks. The sum of three parts of irreversible heat works as an input to a cell thermal mass, which also has continuous heat convection with coolant. The temperature of the cell thermal mass is sensed and sent back to other Simscape blocks.

3.2 Battery Module Modeling

The cell equivalent circuit model is integrated into one block. Eight cell blocks are connected in series to get one battery module model (Figure 3.2). Nine electrical ports are used to connect an external load and balancing circuits. Each cell block sends out its SOC, and states of all cells create a bus signal which will be used in balancing algorithms. The thermal mass inside each cell block has inflow heat because of cell internal resistance and outflow heat because of heat convection with coolant. The coolant temperature is simplified to be same as the before cell temperature and the first cell is cooled by ambient temperature coolant.

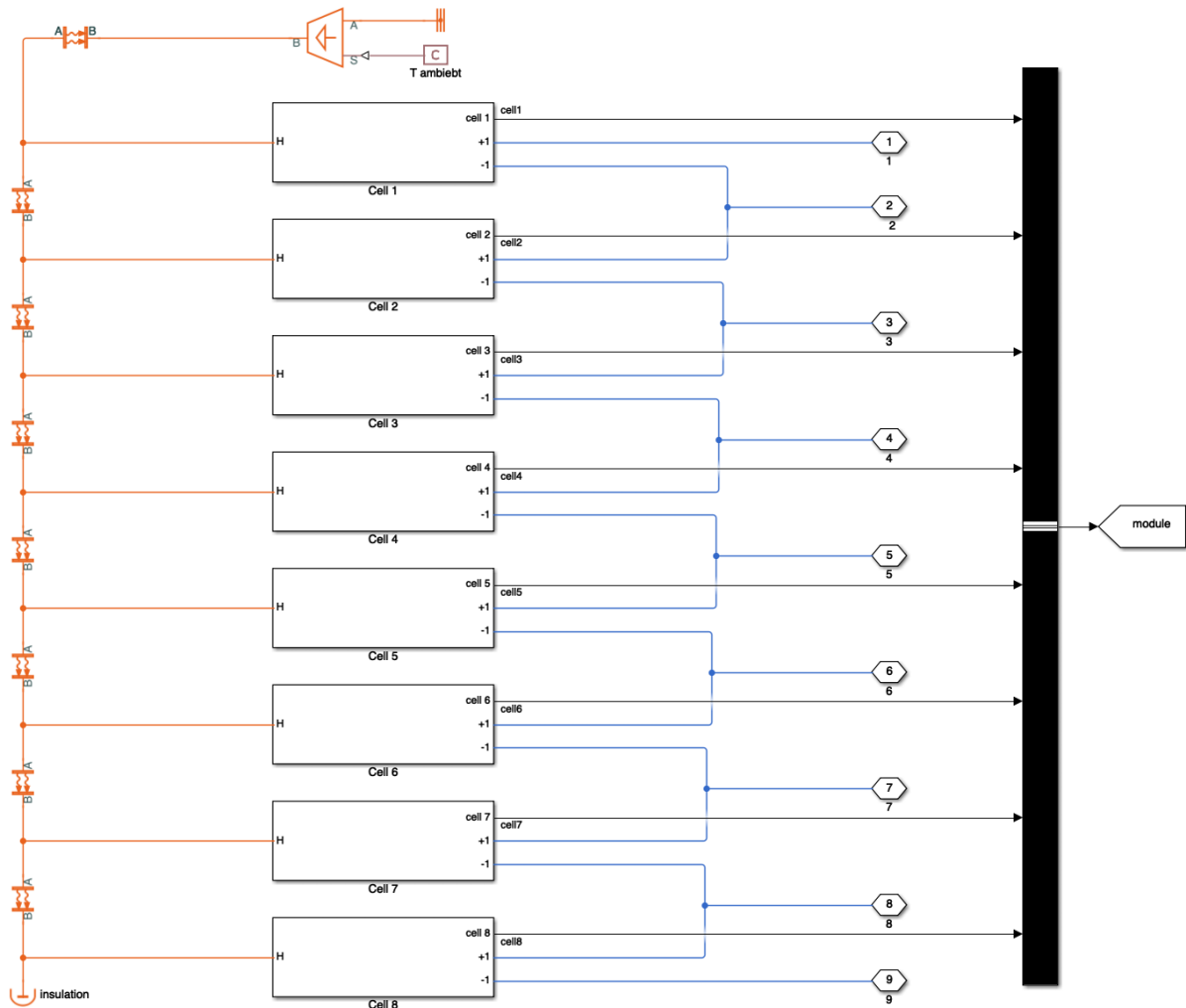


Figure 3.2: Module model

3.3 Complete Battery Modeling

As can be seen in Figure 3.3, the complete battery model consists of four blocks: balancing algorithm block, battery module block, balancing circuit block, and load block. The battery module block is introduced in subsection 3.2 already. The balancing circuit block has balancing electrical components that are connected to the battery module block. The balancing algorithm block has balancing algorithms inside and it also sends out control signals to the balancing circuit block. The load block simulates battery requested power and is connected to positive and negative points of the battery module block. When different balancing methods are modeled, the balancing algorithm block and balancing circuit block need to be changed accordingly.

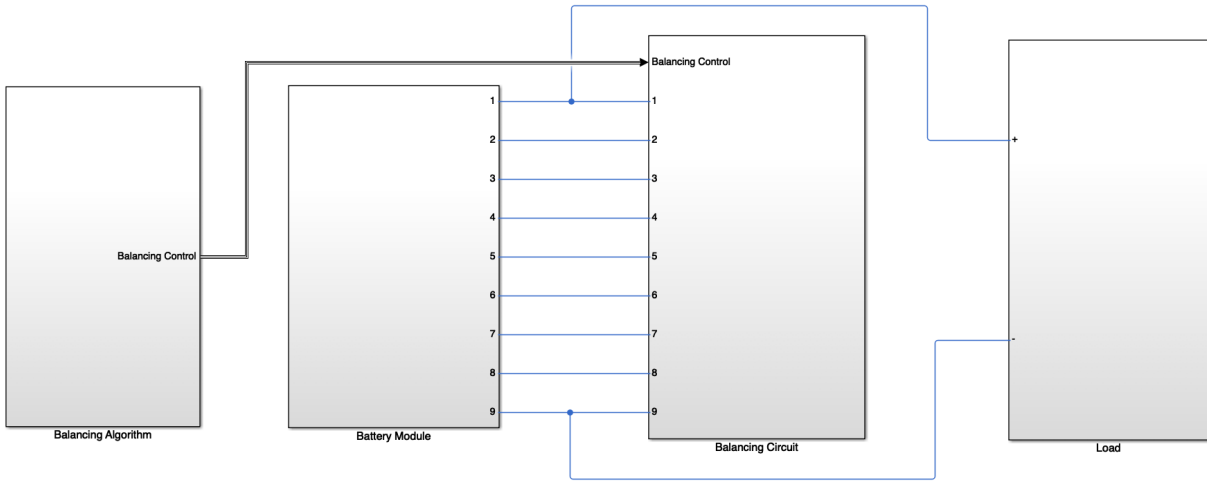


Figure 3.3: Battery model

Figure 3.4 shows one balancing algorithm block. SOC information of all cells is sent to this block, whose values are firstly checked. If any cell has a SOC smaller than 0.01, the simulation will be stopped to avoid any over-discharging. The state-flow is used for coding balancing algorithms.

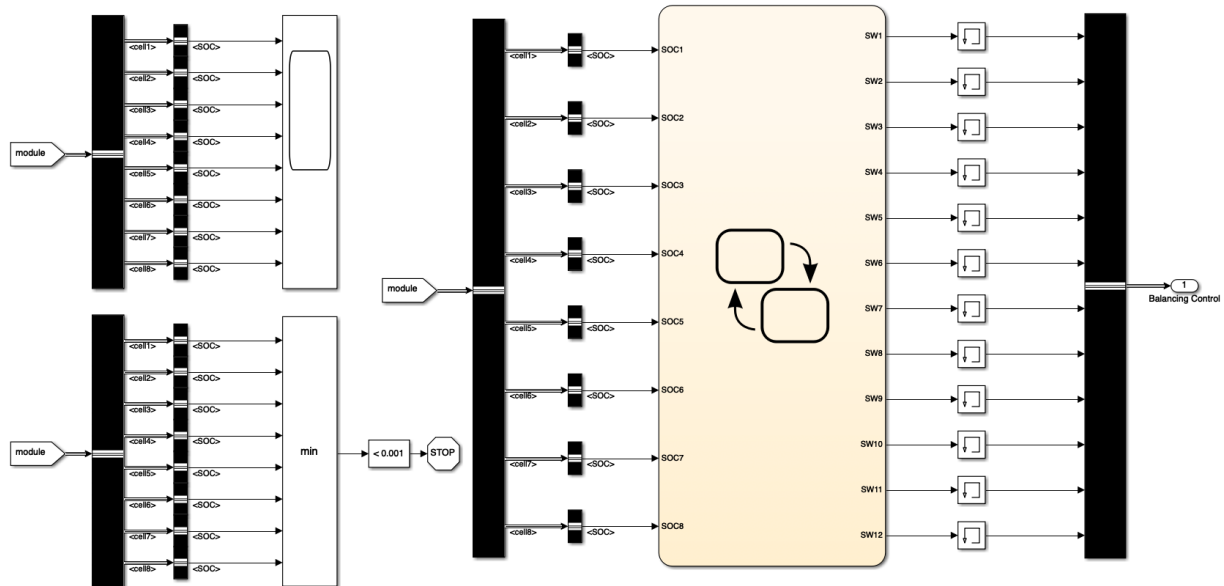


Figure 3.4: Balancing algorithm block

Requested battery power of the WLTC driving cycle can be calculated from vehicle parameters and longitudinal vehicle dynamics explained in subsection 2.1. This power is also scaled down to one battery module amount, which is shown in Figure 3.5. The maximum traction power is about 600 W and the maximum regeneration power is about 300 W.

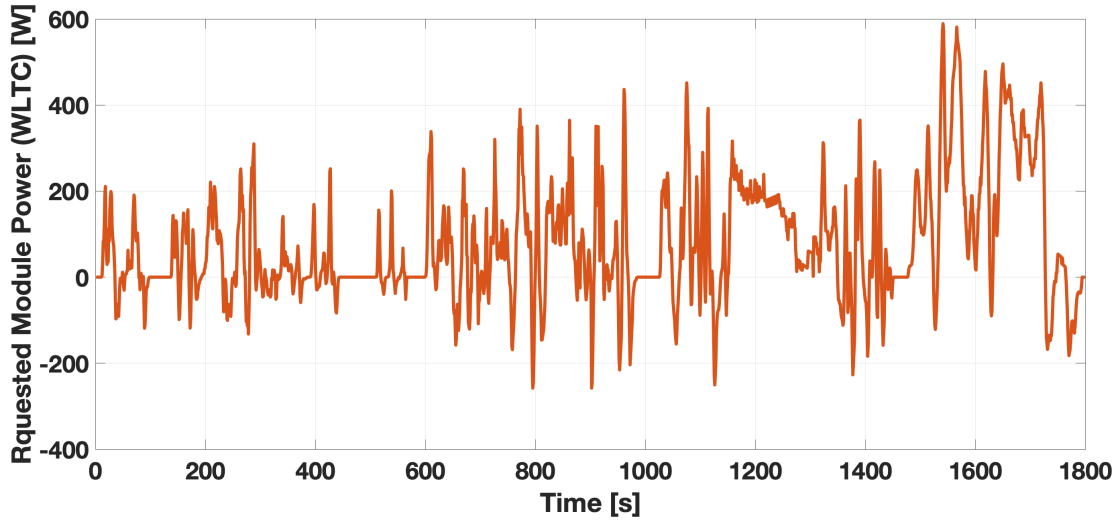


Figure 3.5: Requested module power (WLTC)

A power source Simscape block is used in the load block of the battery model (Figure 3.6). The table of requested power and time has been saved in the power source block. A voltage sensor is used to read the battery terminal voltage. By controlling source currents provided by the power source block, battery charging or discharging power is also controlled.

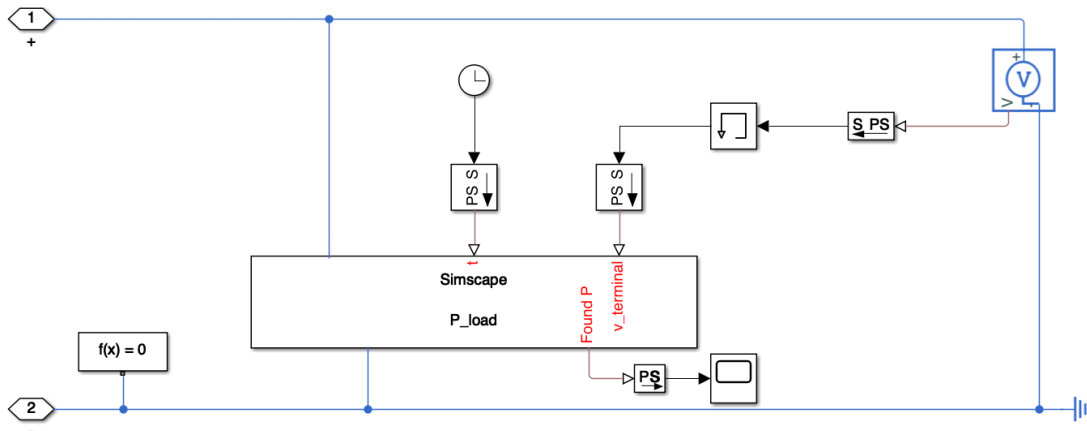


Figure 3.6: Load block

4 Passive Balancing

Passive balancing dissipates the exceeded energy of high SOC cells by parallel connecting shunt resistors. Passive balancing has advantages of low costs, low complexity, and easy control algorithms. But since unbalanced cell energy is totally wasted in the form of heat, cell cycle efficiency is reduced and there are also thermal problems if balancing currents are too high [22].

4.1 Passive Balancing Review

There are two types of passive balancing: *fixed resistor balancing* and *switched resistor balancing*. The biggest difference between these two methods is whether the parallel resistors can be connected and disconnected by controlling switches.

4.1.1 Fixed Resistor Balancing

In the *fixed resistor balancing* (Figure 4.1), each cell has a continuous current passing through its parallel-connected shunt resistor [23]. This method is possible to balance energy levels of cells without any controlling actions because the bypass currents are proportional to cell terminal voltages. However, the bypass currents always exist and bring continuous waste power. Also, the balancing speed of this method is not fast enough. Over-charging and over-discharging easily happen, which is not acceptable in Lithium-ion batteries. Only Lead-acid batteries and Nickel-based batteries are still using this method [24].

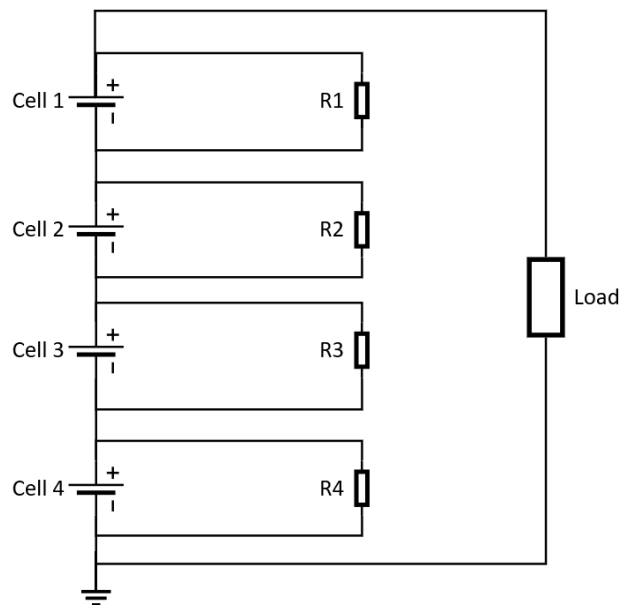


Figure 4.1: Fixed resistor balancing

4.1.2 Switched Resistor Balancing

The *switched resistor balancing* (Figure 4.2) has an additional switch connected to each shunt resistor. During the charging process, when one cell is firstly fully charged the switch parallel connected to that cell will be turned on and a balancing current will pass through the connected shunt resistor. That cell is protected from over-charging, while other cells can be further charged. Only when all cells are fully charged, the charging process will be stopped. During the discharging process, when one cell is fully discharged the battery will stop to provide output power. Switches parallel connected to other cells will be turned on, making exceeded energy dissipated in shunt resistors. Until all cells are fully discharged, the discharging process will be stopped. What's more, cells can also be balanced when there is no charging or discharging current if SOC difference among all cells is found to be larger than a limit value [25][26].

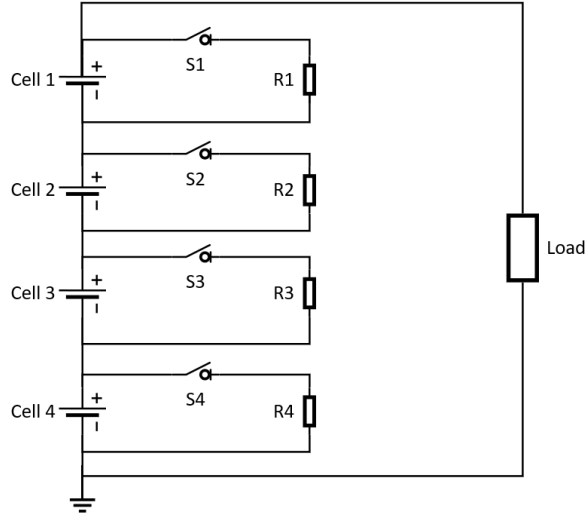


Figure 4.2: Switched resistor balancing

4.2 Passive Balancing Modeling

The complete battery model with the *switched resistor balancing* is created (Figure 4.3). The passive balancing function is activated during the charging process. So the battery model has a charging block where CC-CV (Constant Current-Constant Voltage) charging process is used.

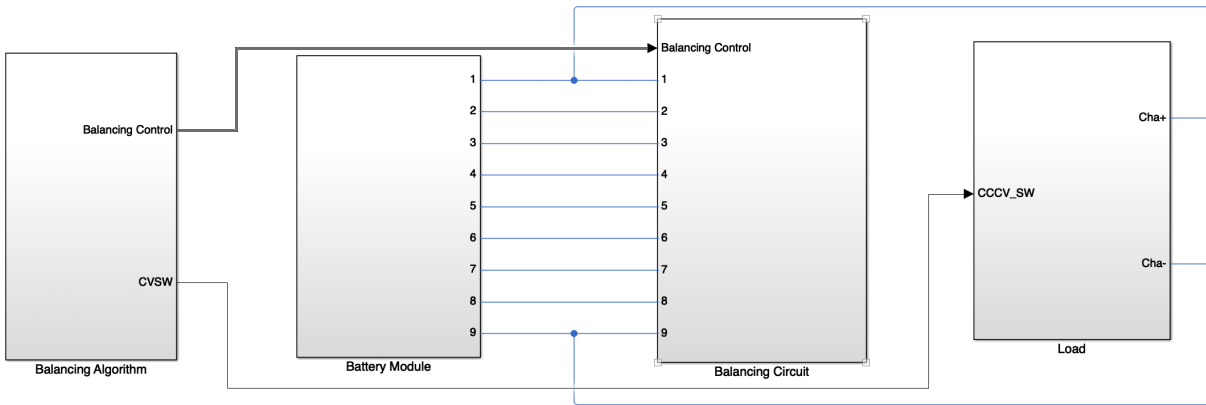


Figure 4.3: Switched resistor balancing, battery model

The balancing algorithm block is shown in Figure 4.4. The state-flow is not used here due to an easy control method. At the beginning of the charging process, a constant current (24 A) is used to charge the battery in a high speed. This fast charging process will be stopped when one cell has its SOC reach 1, and the passive balancing process will be started. The switch connected to the fully charged cell is turned on, series connecting a shunt resistor to it. There will be a dissipating current (around 0.65 A) in the shunt resistor wasting energy in the fully charged cell. At the same time, the charging current is reduced from 24 A to 0.2 A. As a result, the fully charged cell is discharged by around 0.45 A current, and the other cells are charged by 0.2 A current. What's more, a relay block is used in controlling each switch. After the fully charged cell is discharged to the SOC of 0.98, the switch of that cell will be turned off and the cell will be charged again to the SOC of 1 by 0.2 A current. This energy dissipation action can be applied to one or several cells simultaneously, making their SOC fluctuate between 0.98 and 1. And the passive balancing process will be finished when all cells are charged with their SOC bigger than 0.98.

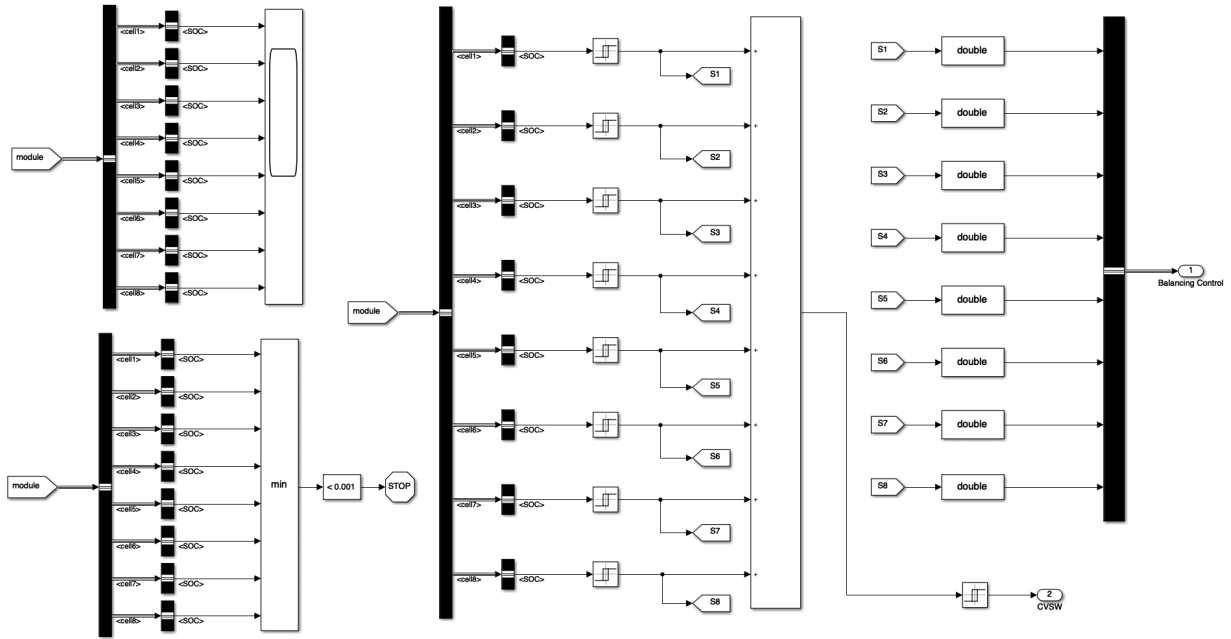


Figure 4.4: Switched resistor balancing, balancing algorithm

The balancing circuit block is shown in Figure 4.5. Each switch is connected to one resistor which can be controlled by bus signals from the balancing algorithm block. The resistor value is set as 6.5Ω to ensure the balancing current is about 0.65 A. If the balancing current is too small the balancing speed will be very slow. If the resistor value is reduced and the balancing current is too big, much heat will be accumulated which may bring thermal problems.

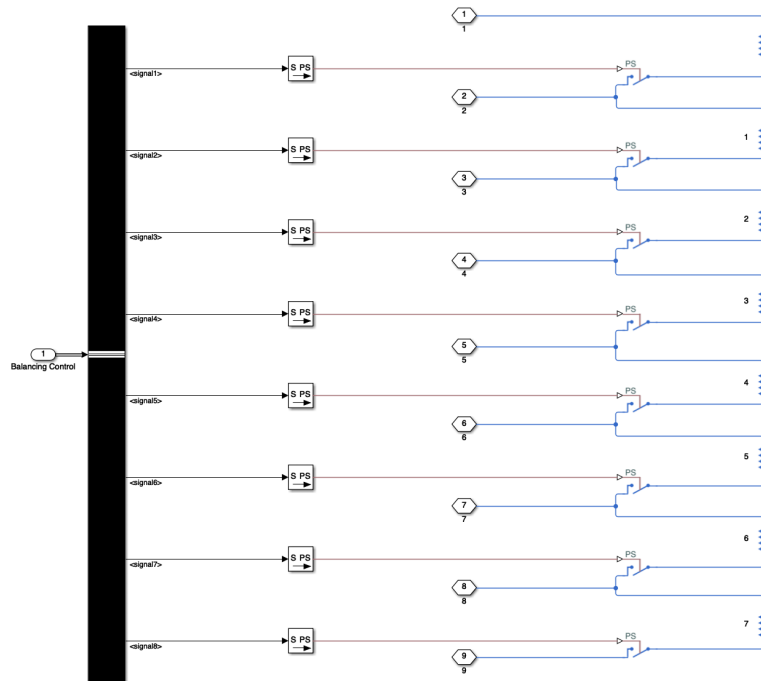


Figure 4.5: Switched resistor balancing, balancing circuit

5 Active Balancing

In order to avoid much energy losses in passive balancing, many active balancing methods have been developed. The main idea of active balancing is to use energy storage components, such as capacitors, inductors, or transformers, to store charges from high SOC cells and transfer them to low SOC cells. Active balancing has the advantage of utilizing battery energy to a much bigger extent, but it always needs more complex configurations and control algorithms [27][28].

5.1 Capacitor Based Active Balancing Review

Capacitor based active balancing uses capacitors as energy storage components, which are normally parallel connected to cells [11]. *Switched-capacitor balancing* was the first one being developed, which has fewer capacitors and easy control algorithms, but its balancing time is quite long especially when more cells are in series connection [29]. In order to improve balancing speed, some structures are added to the *switched-capacitor balancing*, which aims at providing more paths to transfer charges between cells at any position, such as double-tiered structure, chain structure, parallel structure, delta structure, mesh structure, etc. In order to realize modularization design, *modularized switched-capacitor balancing* and *modularized double-tiered switched-capacitor balancing* have also been developed, which use additional capacitors to balance adjacent cell groups. *Single capacitor balancing* can balance the highest SOC and the lowest SOC cells directly, while more complex control algorithms are needed.

5.1.1 Switched-Capacitor Balancing

Switched-capacitor balancing is shown in Figure 5.1. When the balancing process is activated, the same PWM signals are given to all switches and all switches are turned up and down with the same frequency [29]. Each capacitor is connected to two adjacent cells repeatedly, which makes energy from the higher voltage cell transferred to the lower voltage cell. The *switched-capacitor balancing* has a very easy control method which even does not need the cell SOC information. However, the balancing time is quite long which is mainly caused by two reasons. Firstly, when the balancing process is almost finished, the voltage difference between two adjacent cells is very small. This small voltage difference is very hard to charge capacitors and transfer charges. Secondly, within one balancing cycle, energy can only be delivered between two adjacent cells. If energy needs to be transferred between two faraway cells, many balancing cycles will be needed [30].

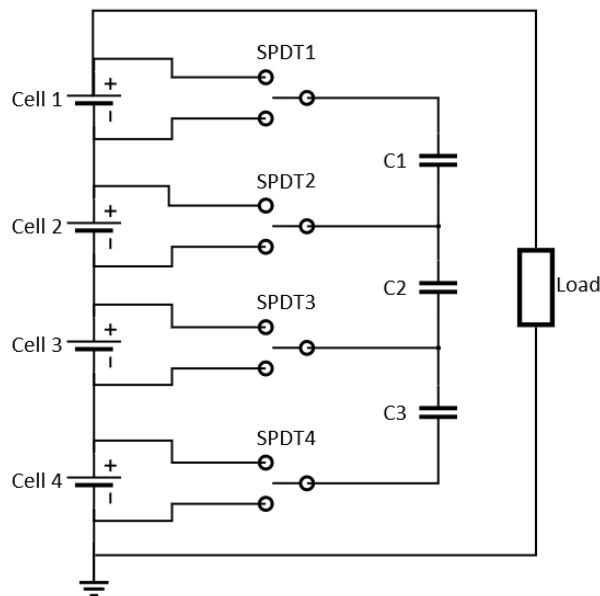


Figure 5.1: Switched-capacitor balancing

5.1.2 Double-Tiered Switched-Capacitor Balancing

Double-tiered switched-capacitor balancing has two layers of capacitors [31]. As shown in Figure 5.2, C1, C2, and C3 are the first layer of capacitors, while C4 and C5 are the second layer of capacitors. The same PWM signals are given to all switches as well. If there is a SOC difference between cell 1 and cell 3, energy can be transferred via C4 directly instead of via C1 and C2. By utilizing these charge-transfer shortcuts, not only can the balancing speed be improved, but also the balancing efficiency can be higher due to fewer times of energy conversion are needed. The disadvantage is more capacitors will be used, which will increase the balancing circuit costs and battery size [30].

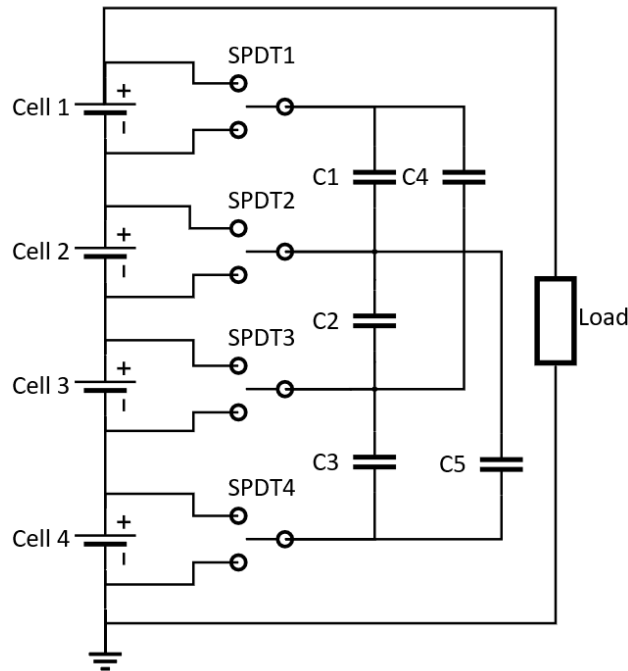


Figure 5.2: Double-tiered switched-capacitor balancing

5.1.3 Chain Structure Switched-Capacitor Balancing

In the *switched-capacitor balancing*, if the first cell and last cell need to be balanced, charges have to pass through every capacitor sequentially. To make this process faster, *chain structure switched-capacitor balancing* has an additional capacitor which connects cells at two ends directly (Figure 5.3). When the balancing is needed, SPDT1-SPDT4 are firstly turned up, SC1 and SC2 are turned on, and SC3 and SC4 are turned off. Secondly, SPDT1-SPDT4 are turned down, SC1 and SC2 are turned off, and SC3 and SC4 are turned on. Cell 1 and Cell 4 are directly balanced with capacitor C0. Adjacent cells are also balanced by C1, C2, and C3. The longest distance between two balanced cells is reduced to half. However, this balancing topology still can not balance two cells at any positions, which means the balancing speed and balancing efficiency will be reduced with the increasing number of series-connected cells [32].

5.1.4 Parallel Structure Switched-Capacitor Balancing

Parallel structure switched-capacitor balancing makes it possible to directly balance two cells at any positions. As shown in Figure 5.4, there is one capacitor connected between cell 1 and any other cells. The balancing operation is the same as the *switched-capacitor balancing*. By using this balancing circuit, any two cells can be connected via one or two capacitors. The balancing speed is thus improved. However, only cell 1 can be balanced with other cells with only one capacitor. Other cell couples have to be balanced with two series-connected capacitors, which will make equivalent resistance higher and bring more energy losses [33].

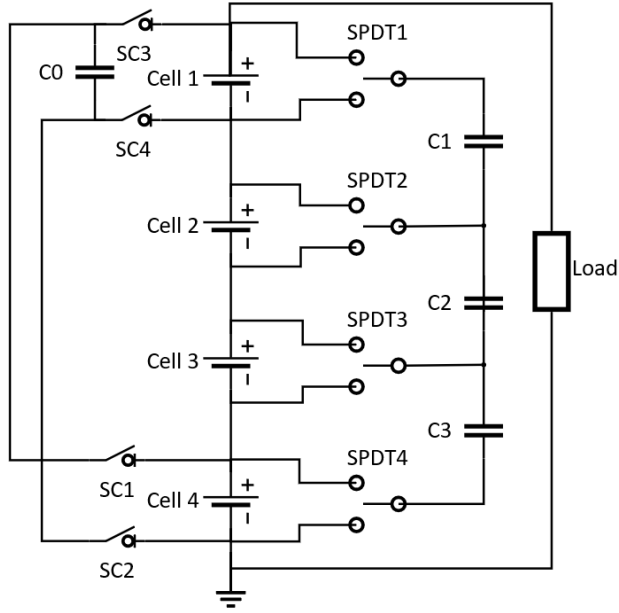


Figure 5.3: Chain structure switched-capacitor balancing

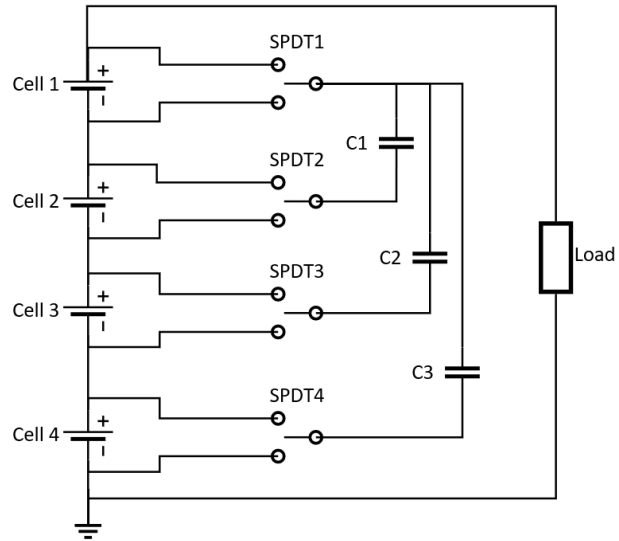


Figure 5.4: Parallel structure switched-capacitor balancing

5.1.5 Series-Parallel Structure Switched-Capacitor Balancing

Series-parallel structure switched-capacitor balancing is able to use the average voltage of all cells to charge or discharge cells (Figure 5.5). During the balancing process, S_{ai} and S_{bi} are firstly turned on, while S_{ci} and S_{di} are turned off (i representing cell numbers). Each cell is parallel connected to one capacitor until they have the same voltage. Secondly, S_{ai} and S_{bi} are turned off, while S_{ci} and S_{di} are turned on. All capacitors are in parallel connection, which makes them be balanced with each other until they share the same voltage. If some cells have lower voltages, the cells will be charged by capacitors when capacitors are parallel connected to these cells again. On the contrary, higher voltage cells will charge the capacitors. This balancing method is not limited by cell positions, but more switches are needed [34].

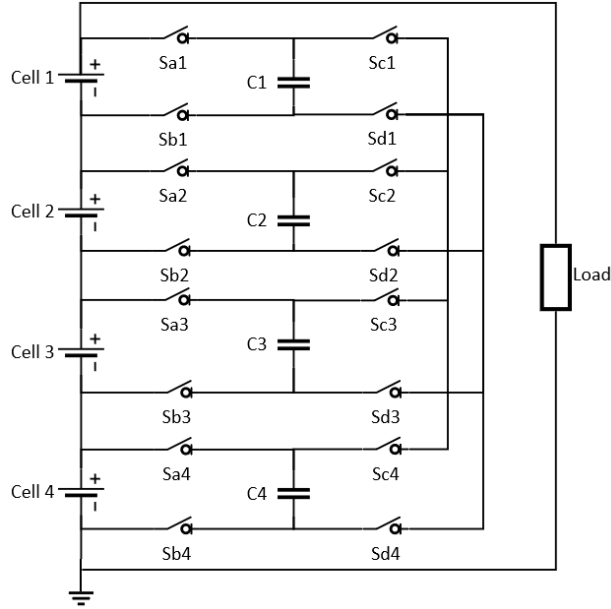


Figure 5.5: Series-parallel structure switched-capacitor balancing

5.1.6 Delta Structure Switched-Capacitor Balancing

Delta structure switched-capacitor balancing gives another way to directly balance two cells at any positions by connecting every cell couple with one capacitor, which is shown in Figure 5.6. This balancing method has a high balancing speed and balancing efficiency. But required capacitors number is $0.5(N^2 - N)$, where N represents the number of series-connected cells. The capacitor number will increase very fast if more cells are connected in series, bringing high costs. What's more, more layers of capacitors are used in the balancing circuit, which also makes battery size bigger [35].

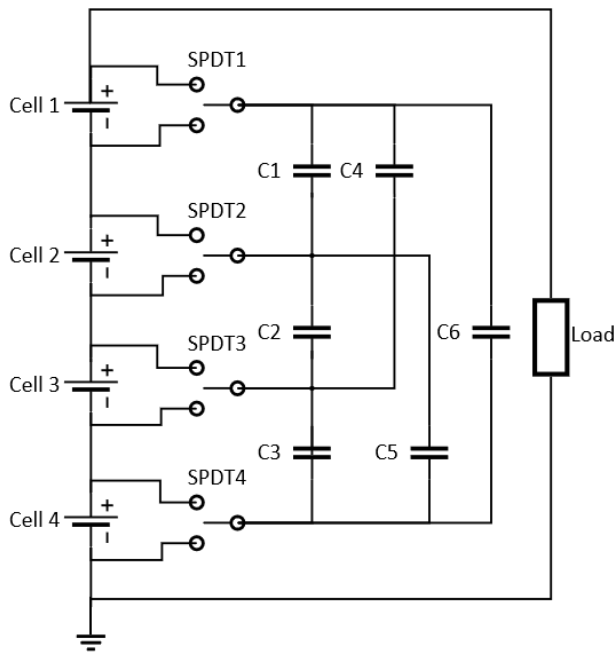


Figure 5.6: Delta structure switched-capacitor balancing

5.1.7 Mesh Structure Switched-Capacitor Balancing

Mesh structure switched-capacitor balancing is shown in Figure 5.7. During the balancing process, the same PWM signals are given to all switches as well, making them turned up and down concurrently. There are paths for adjacent cells and non-adjacent cells to be balanced. Half of the paths have only one capacitor connected between two cells, while the other half of the paths have two capacitors. The total capacitors used in the balancing circuit is $2N$, where N is the number of the series-connected cells. Actually, the mesh structure is a trade-off between the parallel structure and the delta structure. Because it has less energy losses than the parallel structure, at the same time it uses fewer capacitors than the delta structure. But this balancing method still has a rather complex balancing circuit as well as a big battery size [36].

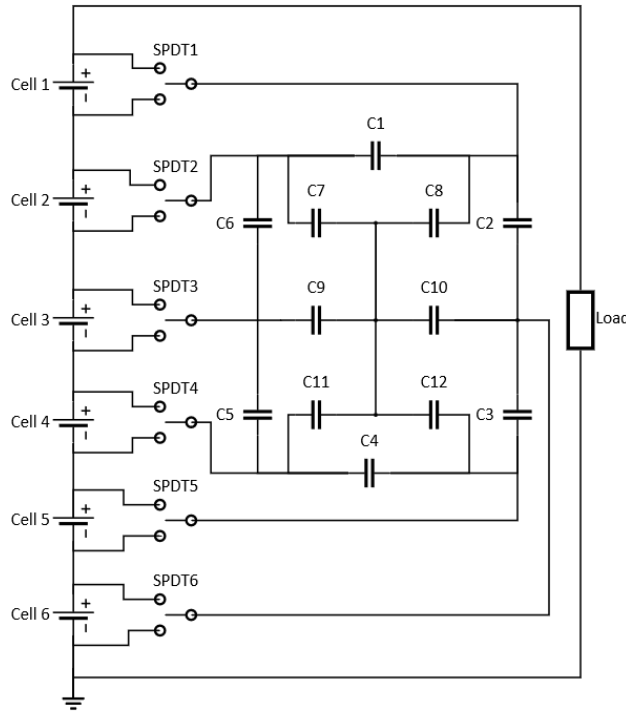


Figure 5.7: Mesh structure switched-capacitor balancing

5.1.8 Chain Structure Double-Tiered Switched-Capacitor Balancing

Chain structure double-tiered switched-capacitor balancing (Figure 5.8) is a combination of the chain structure and double-tiered structure and also has characteristics of both. For this reason, the balancing speed and balancing efficiency are also better than both of them. The balancing operation is the same as the normal chain structure balancing. Since there are two structures used in this balancing method, the costs and battery size are both larger as well [37].

5.1.9 Modularized Switched-Capacitor Balancing

Modularized switched-capacitor balancing is another possible solution to improve balancing performance, as shown in Figure 5.9. During the balancing process, SPDT1-SPDT4 are firstly turned up, Sa1 and Sa2 are turned off, Sb1 and Sb2 are turned on. Secondly, SPDT1-SPDT4 are turned down, Sa1 and Sa2 are turned on, Sb1 and Sb2 are turned off. The balancing process of the *switched-capacitor balancing* is realized. Also, cell 1 and cell 2 are together as cell group 1, which can be balanced with cell group 2 (consisting of cell 3 and cell 4) through the capacitor C0. The balancing speed and balancing efficiency are thus improved by this modularization structure. What's more, this structure is helpful with battery modularization design, especially a large number of cells need to be connected in series [38][39].

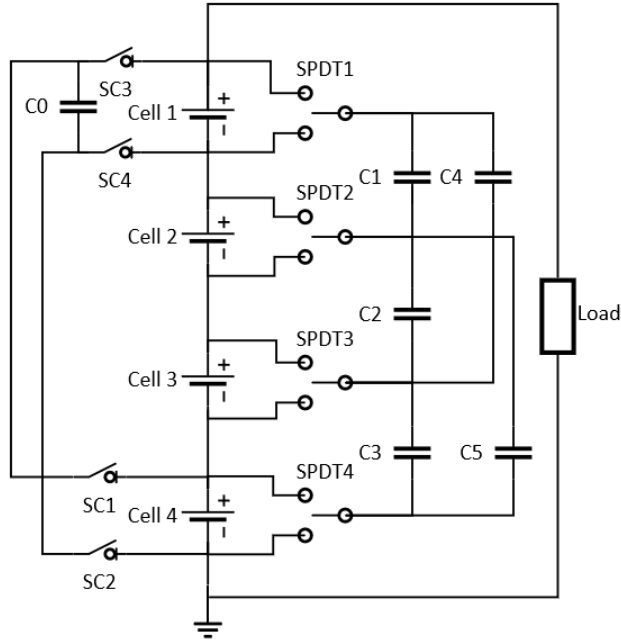


Figure 5.8: Chain structure double-tiered switched-capacitor balancing

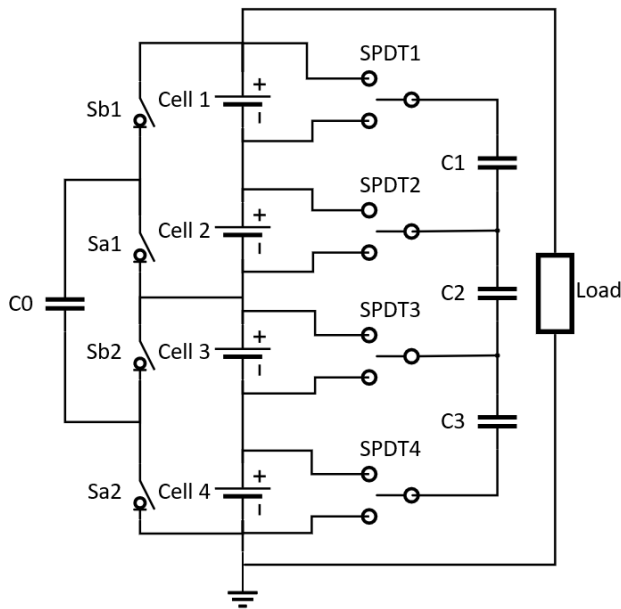


Figure 5.9: Modularized switched-capacitor balancing

5.1.10 Modularized Double-Tiered Switched-Capacitor Balancing

Modularized double-tiered switched-capacitor balancing is an application of the modularization design into the *double-tiered switched-capacitor balancing*. As shown in Figure 5.10, C1, C2, C3 are the first layer of capacitors, and C4, C5 are the second layer of capacitors. C0 is the capacitor used to balance cell group 1 (cell 1 and cell 2) and cell group 2 (cell 3 and cell 4). The balancing operations are the same with the *modularized switched-capacitor balancing*, but the balancing speed and efficiency are further improved because of more capacitors and more balancing paths [39].

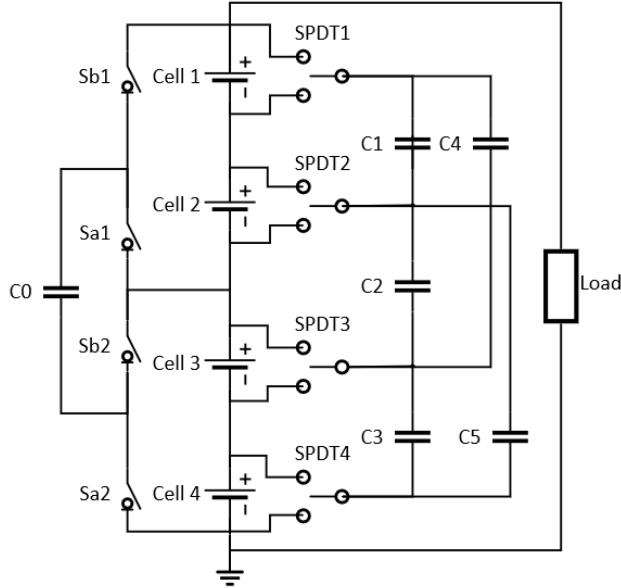


Figure 5.10: Modularized double-tiered switched-capacitor balancing

5.1.11 Single Switched-Capacitor Balancing

Single switched-capacitor balancing (Figure 5.11) has the advantage of more flexible control algorithms. SOC of each cell is calculated and monitored. If the maximum SOC difference among all cells is bigger than a threshold, the balancing process will be activated. The highest and lowest SOC cells are selected out, and turn-on signals are sent to two corresponding switches in order to connect these two cells and the capacitor together. Afterward, SPDT1 and SPDT2 are turned up and down with a certain frequency. Energy from the highest SOC cell is transferred to the lowest SOC cell directly. The balancing process is finished when all cells have a SOC difference smaller than the threshold. The balancing speed of this method will be very fast if only two cells have a big SOC difference no matter which positions these two cells are in. But its balancing time will be much longer if there is a SOC variation among all cells since only two cells can be balanced during one balancing cycle [40].

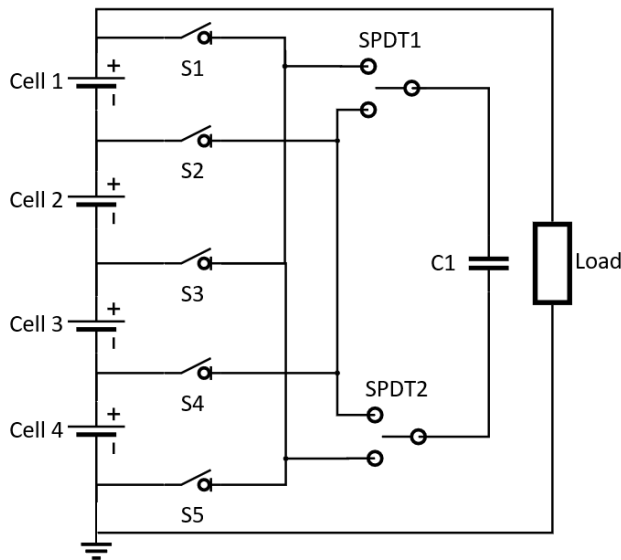


Figure 5.11: Single switched-capacitor balancing

5.2 Inductor Based Active Balancing Review

When current is passing through an inductor, energy is stored in the inductor in the form of magnetic fields. Inductors thus can be used to store and balance energy among cells. Based on different numbers of inductors and switches used in balancing circuits, there are *multi inductor balancing*, *chain structure multi inductor balancing*, *multi tiered inductor balancing*, and *single inductor balancing* [24][28].

5.2.1 Multi Inductor Balancing

Multi inductor balancing (Figure 5.12) can balance many couples of cells synchronously. When the balancing is required between cell 1 and cell 2 with cell 1 having a higher SOC, M1 is firstly turned on while M2 is turned off, and the current starts to charge the inductor L1. After the current of L1 reaches the upper limit, M1 is turned off while M2 is turned on, and the L1 works as an energy source to charge cell 2. Similarly, the L2 and L3 are used to balance cell 2 and cell 3, as well as cell 3 and cell 4. The problem with this method is that only adjacent cells are possible to be balanced directly. When there is a big SOC difference between the first and last position cells, charges shall be transferred via every cell and every inductor, which brings long balancing time and high energy losses due to many times of energy conversion [41].

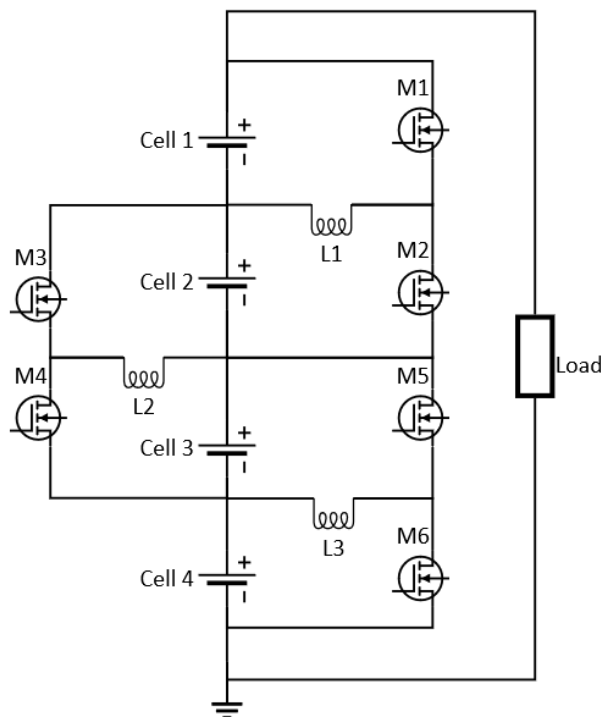


Figure 5.12: Multi inductor balancing

5.2.2 Chain Structure Multi Inductor Balancing

Chain structure multi inductor balancing has an additional capacitor, which is shown in Figure 5.13. The capacitor C0 is used to improve the balancing speed, which can directly connect the first and last position cells. During the balancing process, on-off operations of MOSFETs are as normal to transfer energy between adjacent cells via inductors. At the same time, SC1, SC2 are firstly turned on, and SC3, SC4 are turned off. The C0 is charged by cell 4. Secondly, S1, S2 are turned off, and S3, S4 are turned on, which transfers energy stored in the C0 to cell 1 if cell 1 has a lower voltage (lower SOC). The biggest length between two balanced cells is reduced to half compared to the *multi inductor balancing*. But the balancing circuit size and battery costs are increased [42].

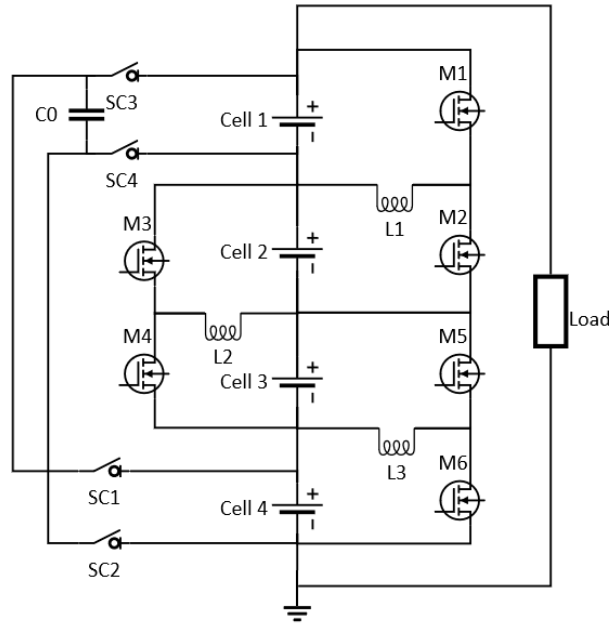


Figure 5.13: Chain structure multi inductor balancing

5.2.3 Multi Tiered Inductor Balancing

Multi tiered inductor balancing (Figure 5.14) provides more paths to transfer charges between cells at different positions. During the balancing process, M1-M7 are firstly turned on while M8-M16 are turned off. The inductors L1-L7 are charged by cell 1, cell 3, cell 5, and cell 7. Afterward, M1-M7 are turned off and M8-M16 are kept off. Energy in L1-L4 is delivered to cell 2, cell 4, cell 6, cell 8 via diodes D8-D11. Energy in L5 and L6 is delivered to cell 3 and cell 4, cell 7 and cell 8 via diodes D12 and D13. Energy in L7 is delivered to cell 5, cell 6, cell 7, and cell 8 via diode D14. There are seven paths that can transfer charges, making the balancing speed faster. But the inductor number will be too many if more cells are connected in series [43].

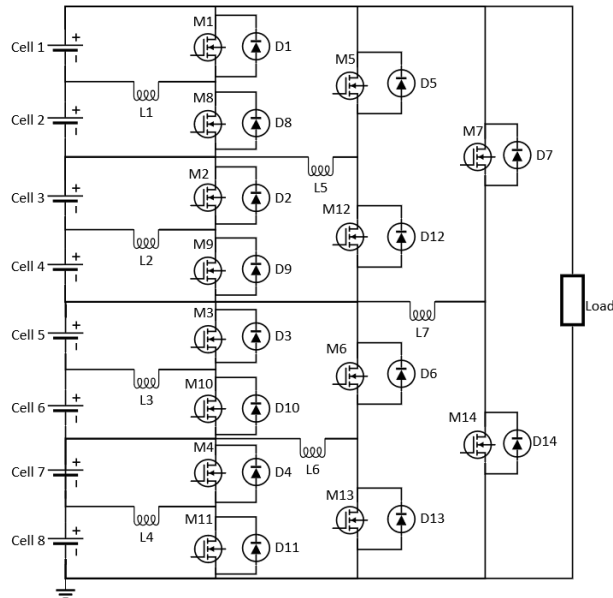


Figure 5.14: Multi tiered inductor balancing

5.2.4 Single Inductor Balancing

Single inductor balancing utilizes one inductor to transfer exceeded energy by controlling different MOSFETs. Based on energy transfer directions, there are two types. This first one is shown in Figure 5.15, which is similar to the *single switched-capacitor balancing*. Energy can be transferred from the highest SOC cell directly to the lowest SOC cell. For example, when cell 1 and cell 2 are the highest and lowest SOC cells respectively, M1 and M1a are firstly turned on, and the current passing through the inductor L keeps increasing to its upper limit. Afterward, M1 is turned off and M2b is turned on, which makes the inductor discharge itself and transfer its energy to cell 2. The second type is shown in Figure 5.16, which uses the complete battery to charge the lowest SOC cell. Cell 6 is assumed to be the lowest SOC cell. M7a and M6b are kept on during the balancing process. The inductor L is charged by the complete battery (cell 1-cell 6) when M1a and M7b are turned on. Afterward, when M1a and M7b are turned off, the energy stored in the inductor will be transferred to cell 6, and cell 6 is charged and balanced. Diodes series connected to MOSFETs in the balancing circuits are used to avoid any possible short-circuits. Both of these two types can select cells and balance them, but the control algorithms are more complex. The balancing speed is medium due to only one or two cells can be balanced during one balancing cycle [44][45].

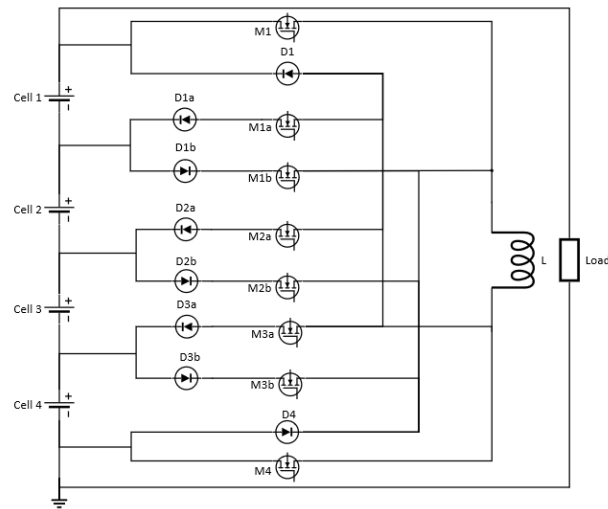


Figure 5.15: Single inductor balancing (cell to cell)

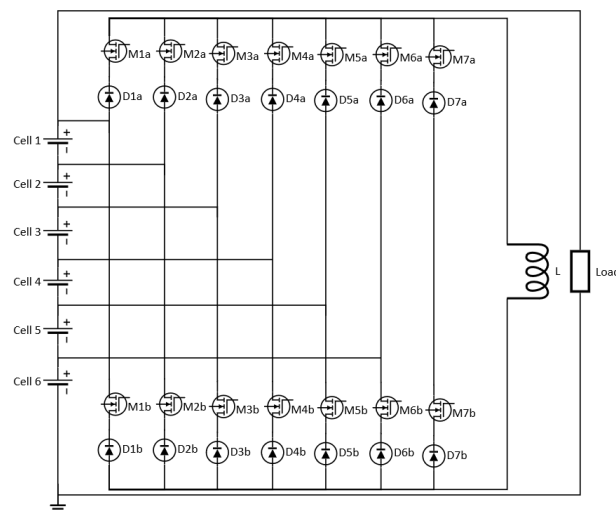


Figure 5.16: Single inductor balancing (battery to cell)

5.3 Converter Based Active Balancing Review

The last active balancing category is converter based active balancing, which includes *boost converter balancing*, *single converter balancing*, *Cuk converter balancing*, *Quasi resonant converter balancing*, *flyback converter balancing*, etc. Converter based active balancing has a really high flexibility of controlling the balancing process, but it is normally more complex and expensive [11][27].

5.3.1 Boost Converter Balancing

As shown in Figure 5.17, each cell is connected to one boost converter. One cell and one boost converter work as an individual cell equalization unit to provide a certain amount of output power. Since all equalization units are connected in series, all converters have the same output current. But output voltages of the converters are different, which are determined by cell voltages and converter voltage conversion ratios. As a result, the output power of each cell is also different. By controlling the voltage conversion ratios of different converters, SOC of cells can also be controlled [46].

The converter voltage conversion ratios are determined based on SOC of all cells. PWM signals are given to MOSFETs in boost converters. By adjusting the duty ratios of the PWM signals, the voltage conversion ratios can also be adjusted. If the maximum SOC difference of all cells is smaller than a threshold value, all MOSFETs are set to off status when no balancing is needed. If this SOC difference is bigger than the threshold value, the balancing process is activated. MOSFETs connected to higher SOC cells will be given higher duty ratio PWM signals, in order to make these cells provide more power. In contrast, cells will lower SOC have smaller duty ratios and smaller output power. When all cells are balanced, the battery will be changed from the balancing mode to the normal mode again when all MOSFETs are turned off again.

It should be mentioned there is an additional switch (S1-S4) connected in every boost converter. They are used for the fault cell bypass function. If one cell is found failed, whose bypass switch will be turned off, and charging or discharging current will not pass that cell anymore. The other converters can be adjusted to have bigger voltage conversion ratios to meet the complete battery output voltage requirement. By utilizing this function, it can be avoided to scrap the complete battery when only one or few cells are damaged. The life-time of the battery is thus significantly improved [46].

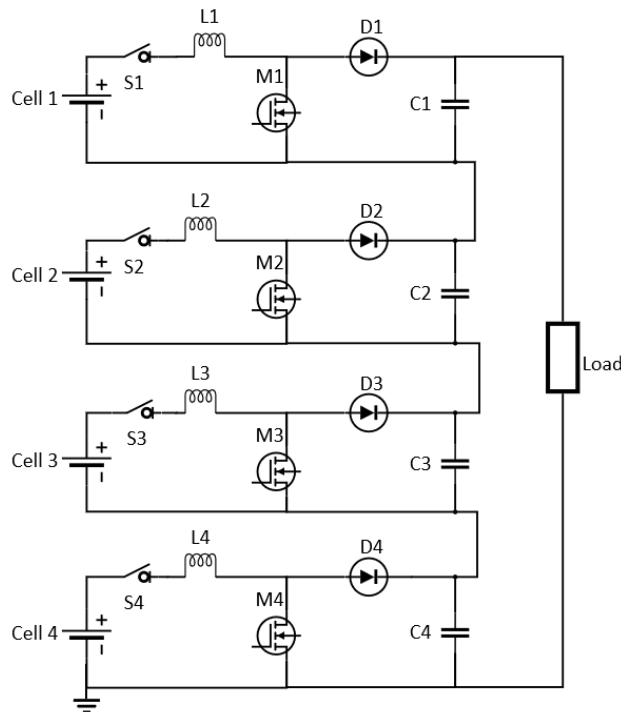


Figure 5.17: Boost converter balancing

5.3.2 Buck Boost Converter Balancing

Buck boost converter balancing (Figure 5.18) has a similar structure to the *boost converter balancing*. One buck boost converter is connected to one cell, working as an individual cell equalization block. Voltage conversion ratios of the buck boost converters and cell output power can be controlled by duty ratios of MOSFET PWM signals as well. Different with the *boost converter balancing*, the voltage conversion ratios can be both bigger than 1 and smaller than 1, making control algorithms more flexible [47][48].

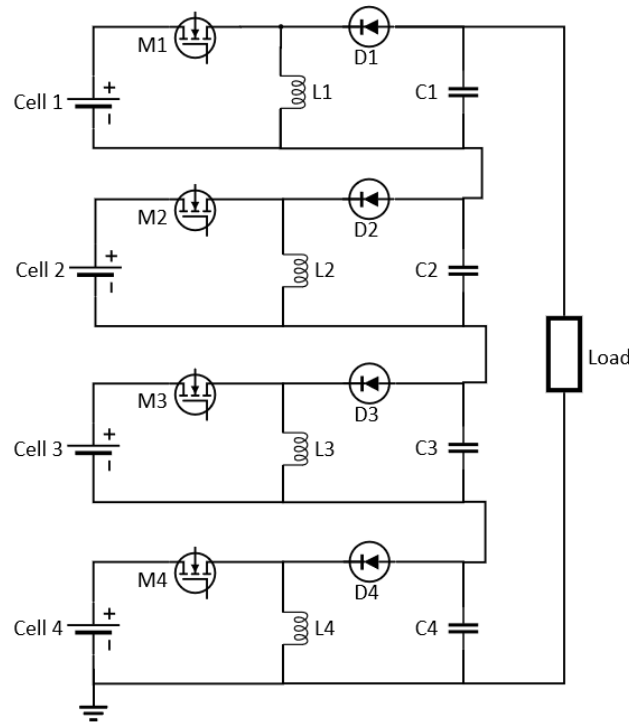


Figure 5.18: Buck boost converter balancing

5.3.3 Single Converter Balancing

Single converter balancing is shown in Figure 5.19, which consists of one DC/DC converter and $4N$ switches (N representing the number of series-connected cells). When balancing is needed, the highest and lowest SOC cells are firstly selected out. The corresponding switches are turned on to connect the highest SOC cell to the source side of the DC/DC converter, while the lowest SOC cell is connected to the DC/DC converter sink side. The DC/DC converter is then operated to transfer energy between these two cells. The efficiency of this balancing method is determined by the DC/DC converter. Energy can be transferred between two cells with the biggest SOC difference directly. However, the balancing time will be long when there is a SOC variation among all cells, since only two cells can be balanced during one period of time [49][50].

5.3.4 Cuk Converter Balancing

Cuk converter balancing has some similar characteristics as *multi inductor balancing*. As shown in Figure 5.20, one cuk converter is connected between any two adjacent cells. If cell 1 has a higher SOC than cell 2, M1 is turned on and off to transfer energy from cell 1 to cell 2. By operating under discontinuous capacitor voltage mode (DCVM), MOSFETs can be turned off while the voltage on it is 0V, significantly reducing switching losses and improving balancing efficiency. But if N cells are connected in series, $(N-1)$ cuk converters will be needed, which is a big cost. What's more, the balancing between none adjacent cells is also slow and needs many times of energy conversion [51][52].

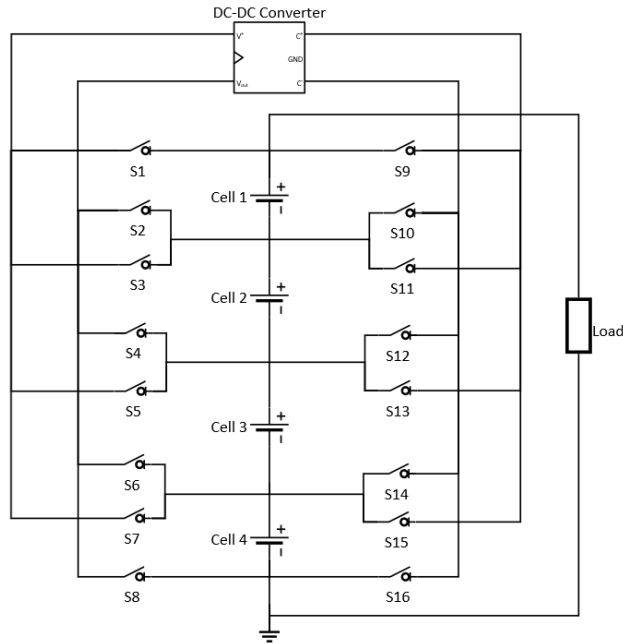


Figure 5.19: Single converter balancing

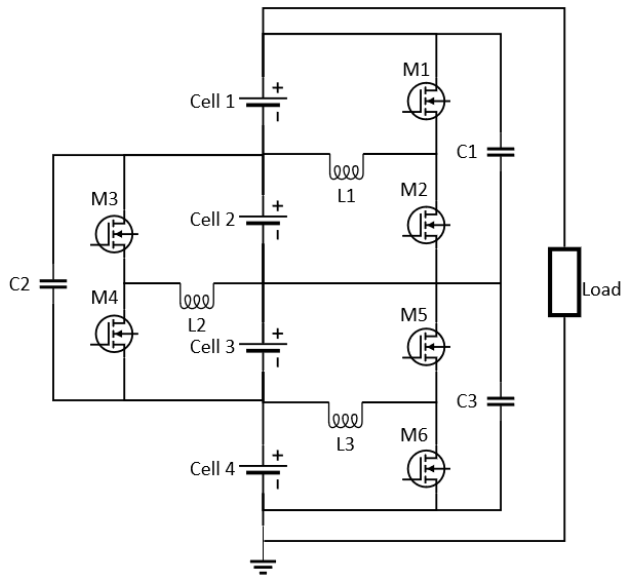


Figure 5.20: Cuk converter balancing

5.3.5 Quasi Resonant Converter Balancing

Quasi resonant converter balancing is shown in Figure 5.21, which has a quasi resonant converter connected between every two adjacent cells. During the balancing process, MOSFETs are controlled by PWM signals to be turned on and off to transfer energy between adjacent cells. In every quasi resonant converter, L_{qi} and C_{qi} work as a resonant tank which can makes MOSFET switching current become 0A. Switching losses and EMI emissions are thus significantly reduced, and balancing efficiency is improved. However, energy transfer between non-adjacent cells is slow and less efficient. One quasi resonant is needed between every two cells, which brings more costs and some packing problems [53][54].

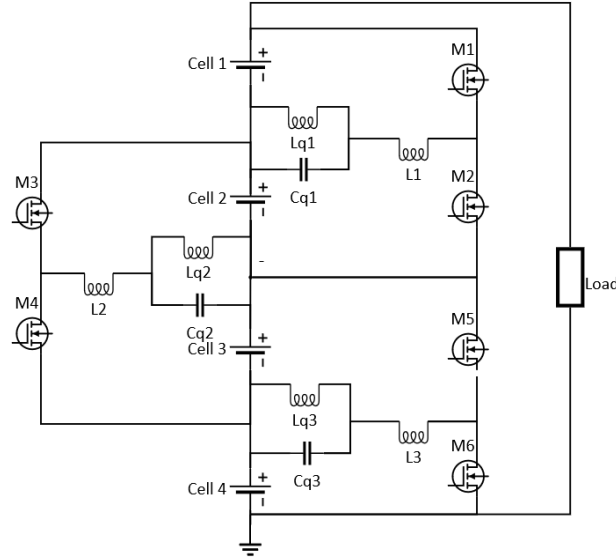


Figure 5.21: Quasi resonant converter balancing

5.3.6 Single Flyback Converter Balancing

Single flyback converter balancing (Figure 5.22) uses one transformer to balance cells. High SOC cells are selected out and used to charge the complete battery via the transformer. For example, when cell 1 has more energy than the other cells, PWM signals will be given to S1 and S2. Firstly, the S1 and S2 are turned on and the current in the transformer increases till its upper limit, which means energy is transferred from cell 1 to the transformer. At this moment, there is no flyback current because of the diode D0. Secondly, the S1 and S2 are turned off and the energy stored in the transformer flybacks to charge the complete battery. Thus, SOC of all the cells are balanced. Other diodes are used to protect cells from any possible short-circuits. Only one flyback converter is used in the balancing circuit, so the costs are relatively low. Balancing is realized between the complete battery and one cell, making its balancing speed faster than the adjacent-cell balancing methods introduced before[55].

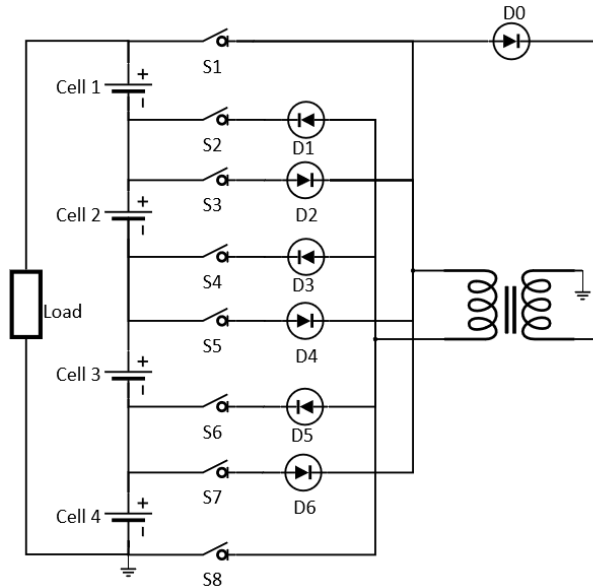


Figure 5.22: Single flyback converter balancing

5.3.7 Multi Flyback Converter Balancing

Multi flyback converter balancing has one flyback converter connected to each cell. As shown in Figure 5.23, the output sides of the flyback converters are connected to cells, while input sides are coupled together and connected across the complete battery. The first cell is assumed to be the lowest SOC cell here. Firstly, S0 and S1 are turned on, and S2, S3, S4 are all kept off. The complete battery starts to charge the transformer until its primary side winding current reaches its maximum value. There is no current in the secondary winding side because of the diode D1. Secondly, S0 is turned off, S1 is kept on, and S2, S3, S4 are all kept off. Energy stored in the transformer flybacks to cell 1. By this way, balancing between the complete battery and the lowest SOC cell is possible. The balancing performance of this method is similar to the *single flyback converter balancing*. But it has more electrical components and higher costs, although *multi flyback converter balancing* is easier for modular balancing block design [56][57].

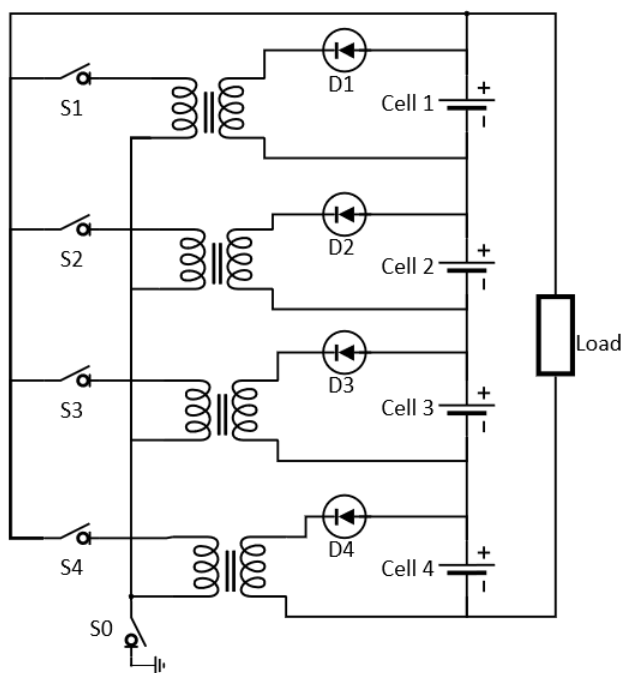


Figure 5.23: Multi flyback converter balancing

5.3.8 Multi Winding Flyback Converter Balancing

Two configurations of *multi winding flyback converter balancing* were found in literature reviews. The first one is shown in Figure 5.24. The primary winding is connected to the complete battery, while each cell is connected to one secondary winding. There are two balancing modes: bottom balancing and top balancing. In the bottom balancing, the complete battery firstly charges the transformer, before the transformer delivers its energy to the lowest SOC cell. In the top balancing, on the contrary, the highest SOC cell firstly charges the transformer, and energy in the transformer then flybacks to the complete battery [58].

The second configuration is shown in Figure 5.25, which has a much easier control algorithm. By turning on S0, the complete battery firstly charges the transformer until the current in the primary winding reaches its upper limit. The S0 is then turned off, and energy stored in the transformer is transferred to all cells. Since all secondary windings have the same turns, if one cell has a lower SOC (lower voltage), the charging current to that cell will be bigger. Similarly, charging currents to high SOC cells are smaller. All cells are balanced by these different currents. However, balancing performance is limited by the different leakage inductance of secondary windings. For both configurations, it is hard to have many secondary windings coupled with a common core, and a large magnetic device has bigger leakage inductance and more energy losses. The packing of the *multi winding flyback converter* is also a problem due to the big core size [59].

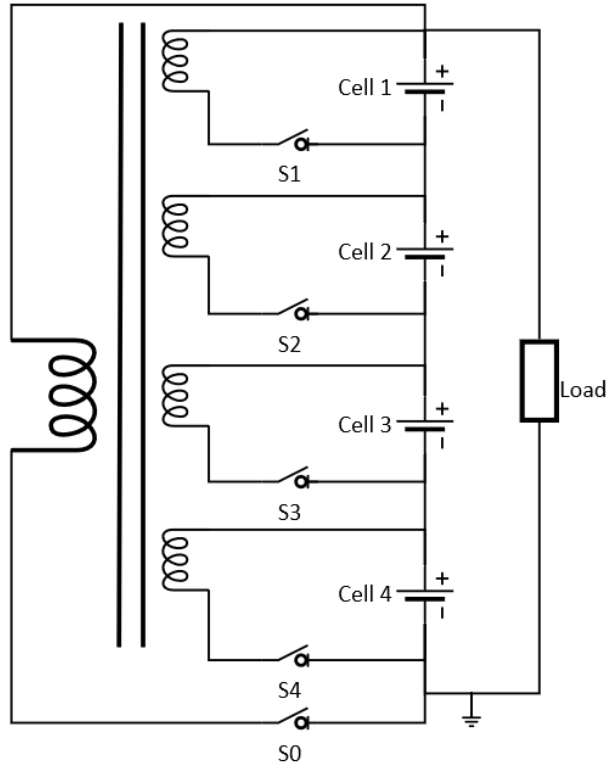


Figure 5.24: Multi winding flyback converter balancing (type 1)

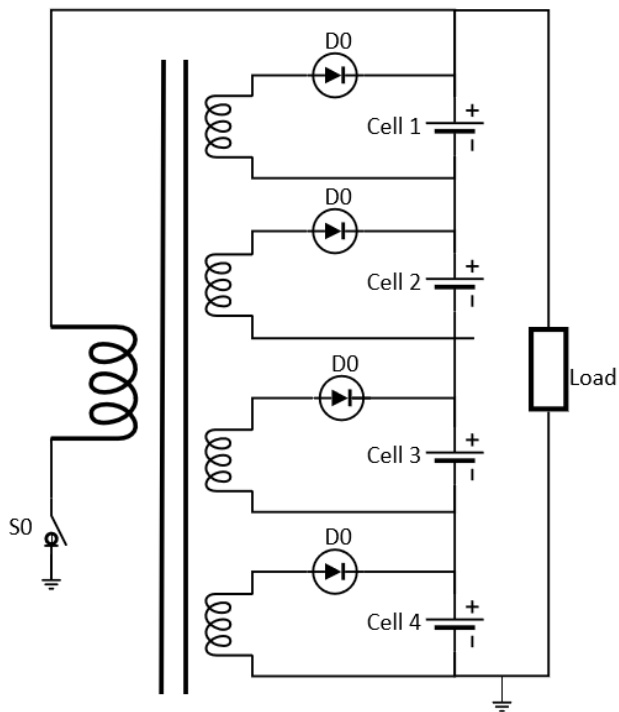


Figure 5.25: Multi winding flyback converter balancing (type 2)

5.4 Active Balancing Modeling

5.4.1 Single Switched-Capacitor Balancing Modeling

As explained in the subsection 5.1.11, the *single switched-capacitor balancing* uses only one capacitor to balance all cells, which has the advantages of small size and low costs. However, if only the highest and the lowest SOC cells are selected and balanced with the capacitor, the balancing speed will be very slow. This is because the small voltage difference between these two cells, which makes balancing current passing through the capacitor also at a quite low level. To solve this problem, the balancing process can be carried out between the battery module and the lowest SOC cell [60]. The battery model described in subsection 3.3 is adjusted by changing the balancing circuit block and the balancing algorithm block, which are shown in Figure 5.26 and Figure 5.27 respectively.

As can be seen in Figure 5.26, there are twelve switches and one capacitor in the balancing circuit. S1-S9 are used to control which cell shall be parallel connected to the capacitor. Positive sides and negative sides of all cells are coupled separately and connected to two terminals of S10 and S11. These two switches are also connected to the positive and negative sides of the capacitor. By turning up and down of the S10 and S11, it can be ensured that the capacitor delivers energy from the battery module to one selected cell. The switch S12 is used to avoid short circuits when the capacitor is under charging.

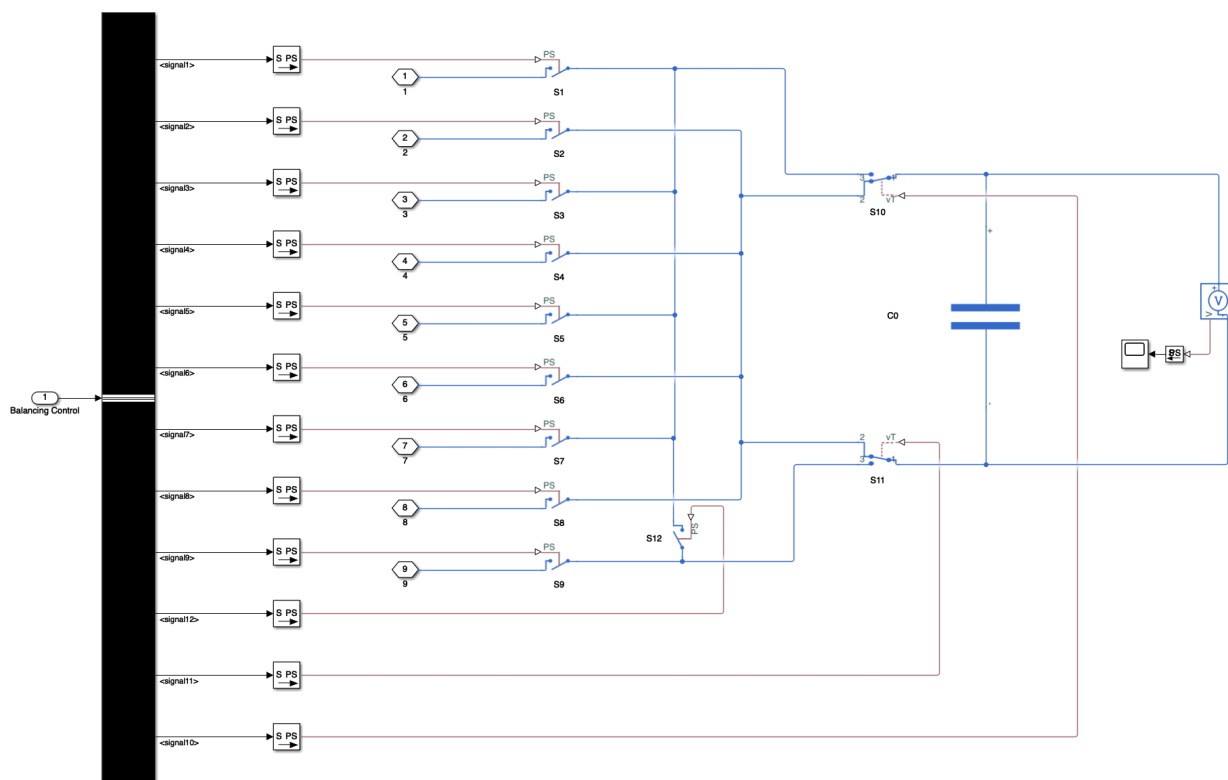


Figure 5.26: Single switched-capacitor balancing, balancing circuit block

Balancing algorithms in the state-flow are shown in Figure 5.27. SOC of all cells are kept being monitored. If the maximum SOC difference is bigger than 0.1%, the balancing process will be activated. During every balancing cycle (5s), there are two steps which are capacitor charging (2.5s) and capacitor discharging (2.5s). During the capacitor charging, S1 and S9 are turned on, S10 is turned up, and S11 is turned down. The complete module is connected to the capacitor and charge it with the module voltage. S12 is turned off to avoid module short-circuit during the capacitor charging process. During the capacitor discharging, the lowest SOC cell is firstly selected out and two switches next to it are turned on. When the cell position is an odd number, S10 and S11 are both turned up. On the contrary, S10 and S11 are turned down if the cell position is an even number. S12 is turned on during the capacitor discharging process. This operation is to

make sure the positive side of the capacitor is connected to the positive side of the selected cell and the cell is charged by the capacitor. After every time of capacitor charging and discharging, SOC of all cells will be checked again to determine the cell to be balanced during the next balancing cycle. If the SOC difference of all cells is found to be smaller than 0.1%, the balancing process will be stopped.

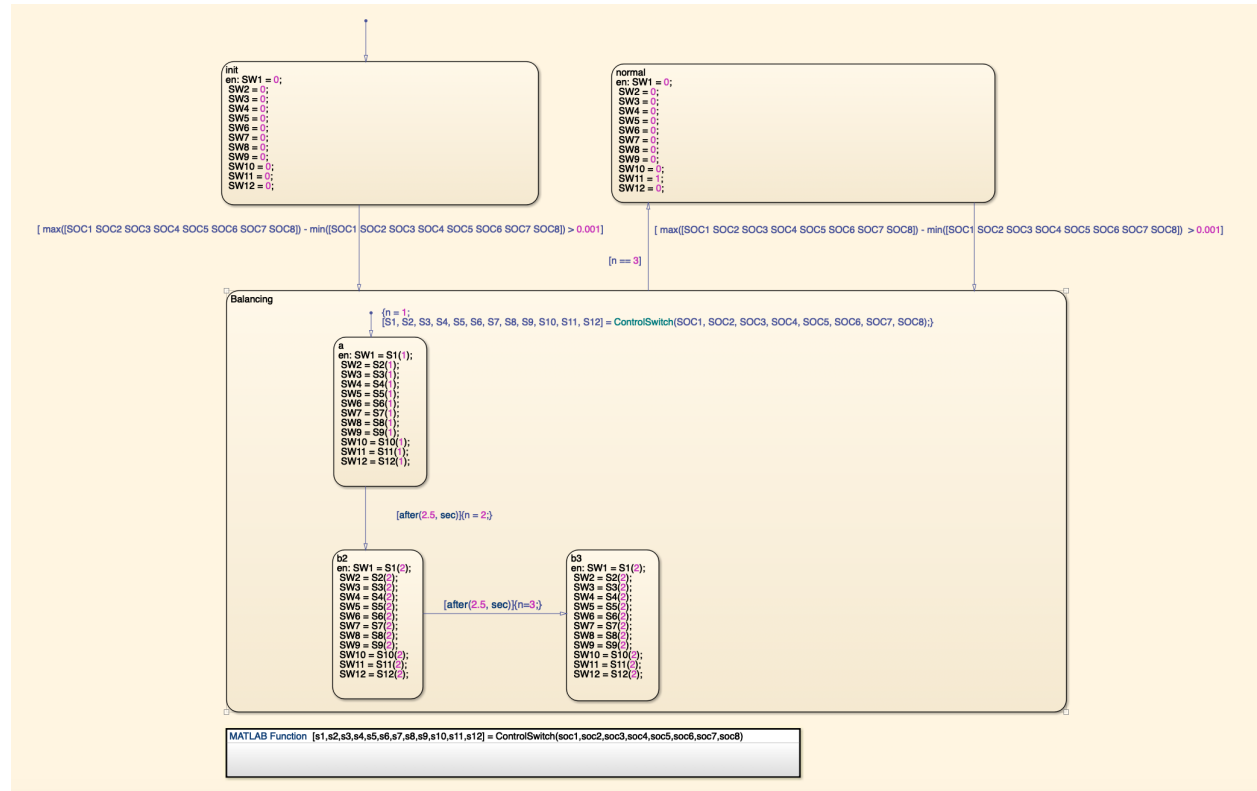


Figure 5.27: Single switched-capacitor balancing, balancing algorithms

5.4.2 Multi Inductor Balancing Modeling

The *multi inductor balancing* has an inductor connected between every two adjacent cells. Compared to capacitor based active balancing methods, it has bigger balancing currents which can significantly improve the balancing speed. Since only eight cells are seriously connected in one battery module, it is sufficient to balance only two adjacent cells in one balancing cycle. If more couples of cells are balanced together, control algorithms will be much more complex and bring less improvement.

The balancing circuit block is shown in Figure 5.28. Seven inductors (L1-L7) are energy storage components. Every two switches are placed up and down of each inductor, which are used to connect the inductor with the upper or lower cell. One bus signal is sent from the balancing algorithm block and controls operations of fourteen switches (S1-S14). Each inductor is series connected with a current sensor, and sensed currents form a bus signal which is given back to balancing algorithm block to realize a closed-loop control.

The state-flow of the *multi inductor balancing* is shown in Figure 5.29. The balancing process is activated when the maximum SOC difference is bigger than 0.1%. The function "ControlSwitch" is used to calculate the SOC difference between every couple of adjacent cells and select out the biggest one, which can determine which cell couple is to be balanced. During every balancing cycle (consisting of two steps), two switches are controlled to be turned on and off while other switches are all kept off. In the first step, the switch connected to the higher SOC cell is turned on while the other is turned off. The cell with more energy starts to charge the inductor. Since the inductor current value is sent from the balancing circuit block, the inductor charging process stops when the current reaches its upper limit (30A). In the second step, two switches both change states, and the inductor starts to charge the lower SOC cell until the inductor current is sensed to reach 0A. In the next balancing cycle, the cell couple to be balanced is determined by the updated SOC distribution.

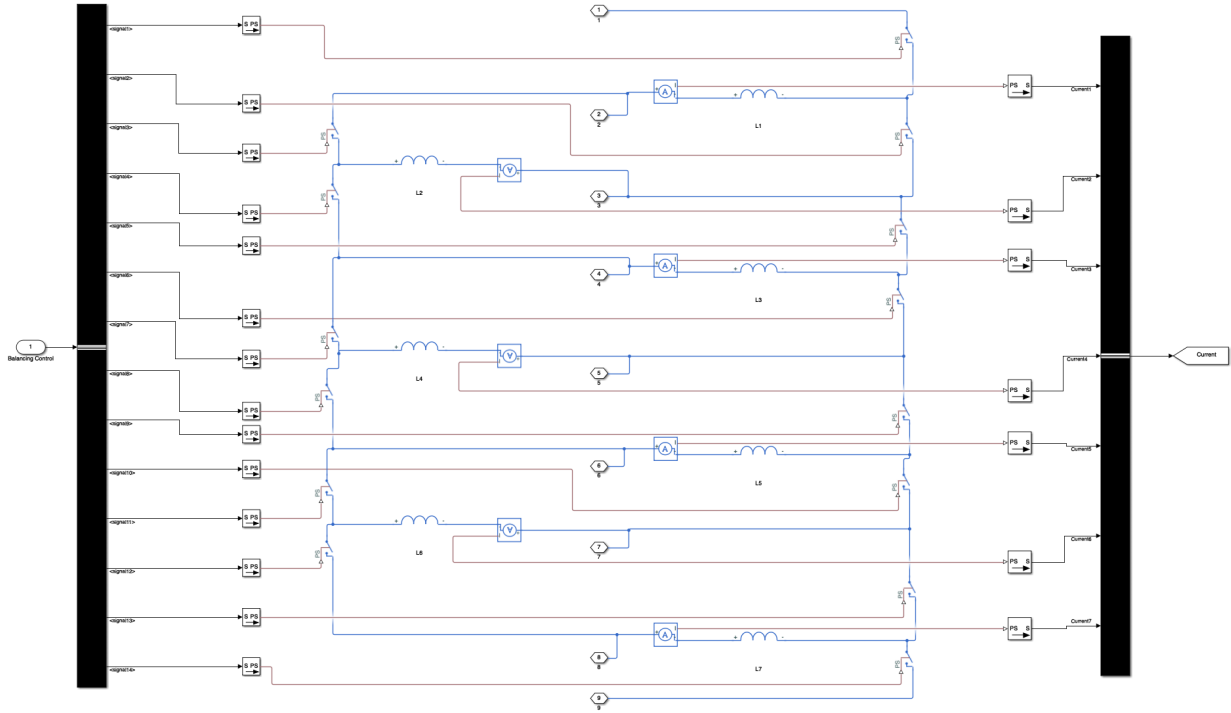


Figure 5.28: Multi inductor balancing, balancing circuit block

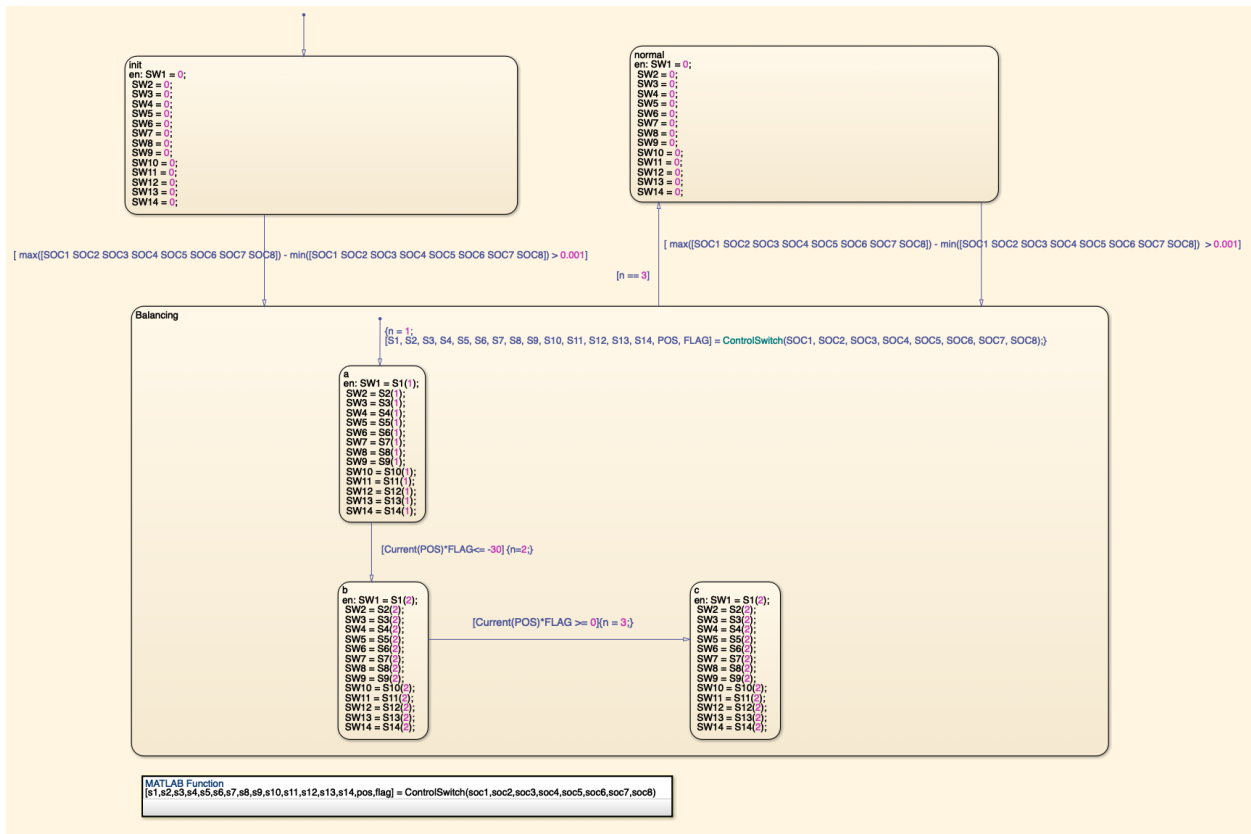


Figure 5.29: Multi inductor balancing, balancing algorithms

The balancing algorithms introduced above are able to control balancing currents fluctuate between 30A and 0A, which can not only avoid overcurrent in inductors but also avoid energy in low SOC cells being transferred back to inductors. In order to realize this function, two additional values need to be calculated in the function "SwitchControl". The first value "POS" determines which inductor is under using for balancing, so that the correct current sensor is used. The second value "FLAG" determines the upper or lower cell has a greater SOC-level. Since each inductor is used to bi-directionally balance two cells and the balancing current can be in two different directions. The value "FLAG" is used to decide the sign of the current limit.

5.4.3 Buck Boost Converter Balancing Modeling

In the *buck boost converter balancing*, each cell together with one buck boost converter works as an individual cell equalization block to provide output power. The balancing circuit block is shown in Figure 5.30. Eight PWM signals are used to control the operations of eight MOSFETs, which are sent from the balancing algorithm block. By controlling the duty ratios of the PWM signals, voltage conversion ratios of the buck boost converters can be controlled. Since unbalanced charges are not delivered among cells in this balancing method, the balancing process can only be activated during the charging or discharging process.

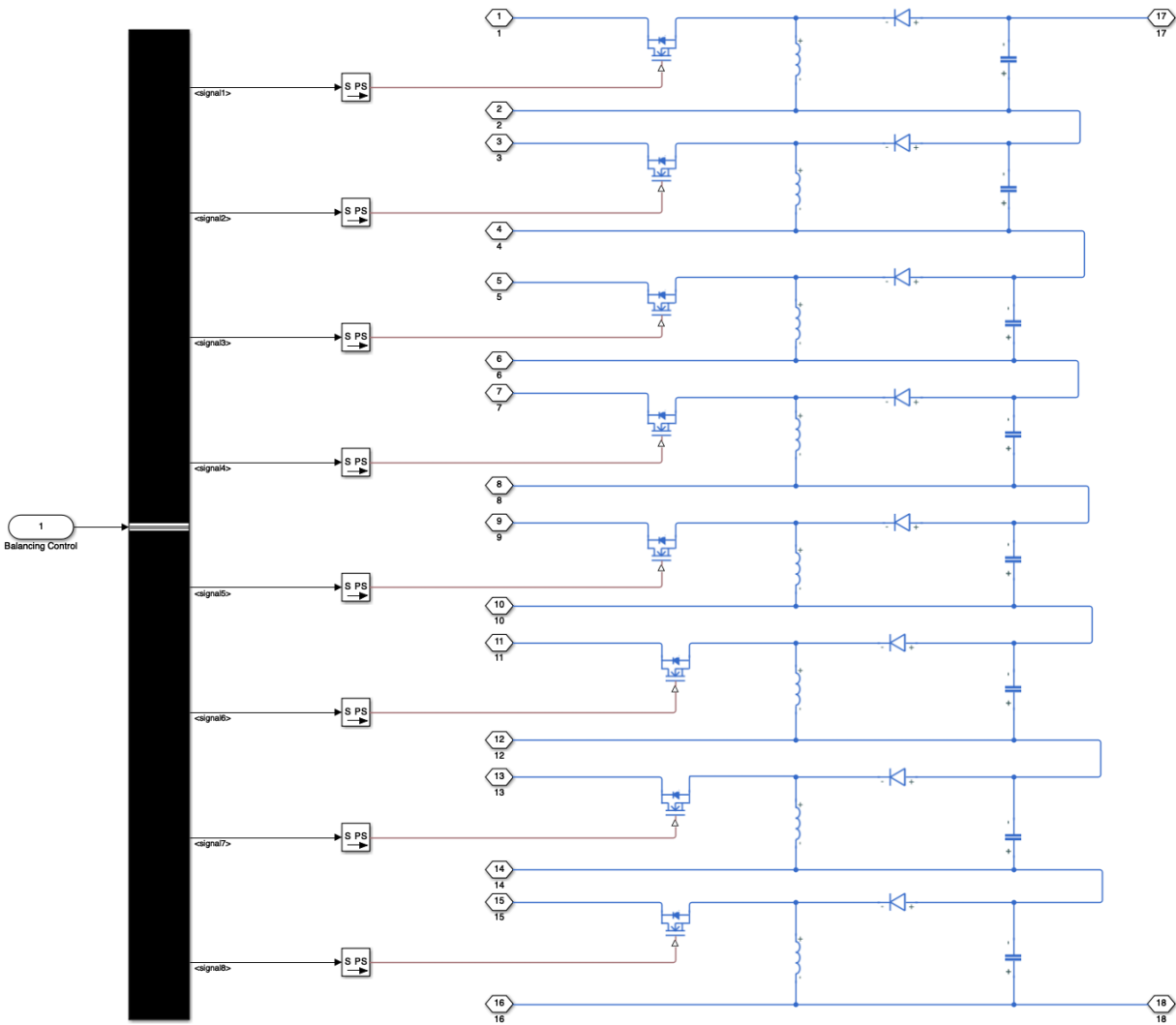


Figure 5.30: Buck boost converter balancing, balancing circuit block

The frequency of the PWM signals is 20Hz, and this high frequency makes the simulation speed very slow. In order to have a better observation of balancing performance, the nominal capacity of cells is reduced to 24mA in the battery model of *buck boost converter balancing*. State-flow in the balancing algorithm block is shown in Figure 5.31, which balances eight cells during the discharging process. If SOC difference among all cells is bigger than 0.1%, the balancing process will be activated. During every balancing cycle (0.05ms), there are four periods (0.01ms, 0.012ms, 0.015ms, 0.0125ms). In the function 'ControlSwitch', the highest and lowest SOC cells are found. MOSFET of the lowest SOC cell is only turned on during the first period, while MOSFET of the highest SOC cell is turned on during the first three periods. MOSFETs of other cells are turned on during the first two periods. By controlling in this way, duty ratios of the highest, middle, and lowest SOC cells are calculated in Equation 5.1, Equation 5.2, and Equation 5.3. And the sum of eight duty ratios are approximately equal to 8, which is to ensure the total module output voltage has small difference compared to the one without balancing.

$$DR_{highest} = \frac{DT}{(1-D)T} = \frac{0.01 \text{ ms}}{0.05 \text{ ms} - 0.01 \text{ ms}} = 0.25 \quad (5.1)$$

$$DR_{middle} = \frac{DT}{(1-D)T} = \frac{0.022 \text{ ms}}{0.05 \text{ ms} - 0.022 \text{ ms}} = 0.78 \quad (5.2)$$

$$DR_{middle} = \frac{DT}{(1-D)T} = \frac{0.0375 \text{ ms}}{0.05 \text{ ms} - 0.0375 \text{ ms}} = 3 \quad (5.3)$$

In the state-flow, it can also be found that after fifty times of balancing cycles (2.5ms period), the balancing process will be interrupted in order to check the updated cell SOC distribution. By running the function 'ControlSwitch' again, the cells to be faster or slower discharged are updated, which will be applied during the next 2.5ms period.

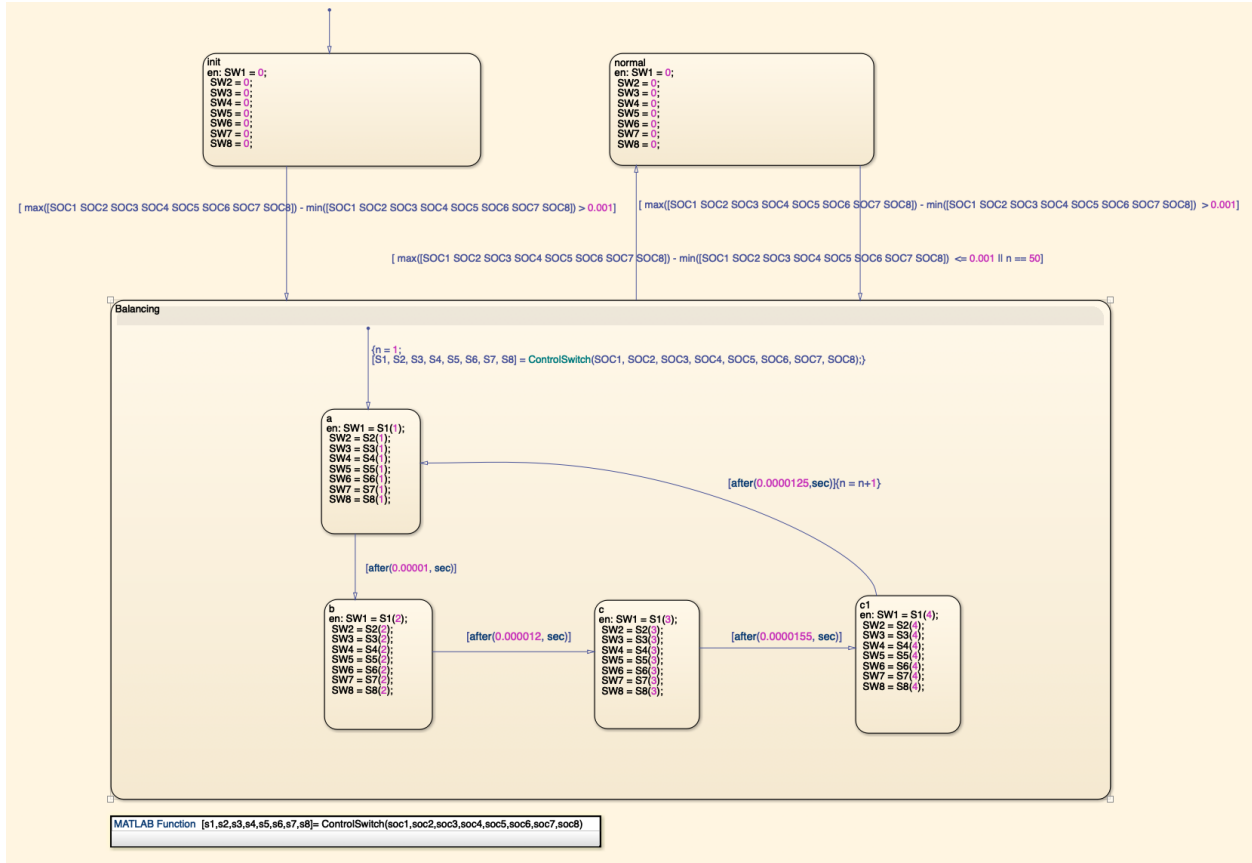


Figure 5.31: Buck boost converter balancing, balancing algorithms

6 New Proposed Active Balancing

Most active balancing methods have the balancing strategy to store energy from higher SOC cells into some energy-storage components and then deliver the energy to lower SOC cells. But this brings losses due to many times of energy conversion. Regeneration is one basic function of PHEVs or BEVs which utilizes generators and converts braking energy into electrical energy. By integrating the regeneration process and balancing process together, the regeneration power can be used to charge energy-storage components in balancing circuits directly, reducing energy conversion times and improving balancing efficiency.

6.1 Balancing Circuit

The balancing circuit (Figure 6.1) is created based on the *single capacitor balancing* by adding one switch next to each cell. Due to a large amount of recovered energy, the normal capacitor is replaced by one supercapacitor to avoid higher switching losses. During the regeneration process, the supercapacitor can replace the highest SOC cell and be charged together with other cells. For example, cell 1 is assumed to have the most energy. When a vehicle is decelerating and there is charging current, S10 is turned off while S11-S17 are turned on, disconnecting cell 1 from the battery series. At the same time, S1-S2 are turned on, S3-S9 are turned off, SPDT1 is turned up, and SPDT2 is turned down, connecting the supercapacitor with other cells. When the battery is providing traction power, all cells are connected in series again by turning off S1-S9 and turning on S10-S17. It should be mentioned that SPDT1 and SPDT2 should not be put in the same position. Otherwise, the supercapacitor will have a short-circuit and be fast discharged.

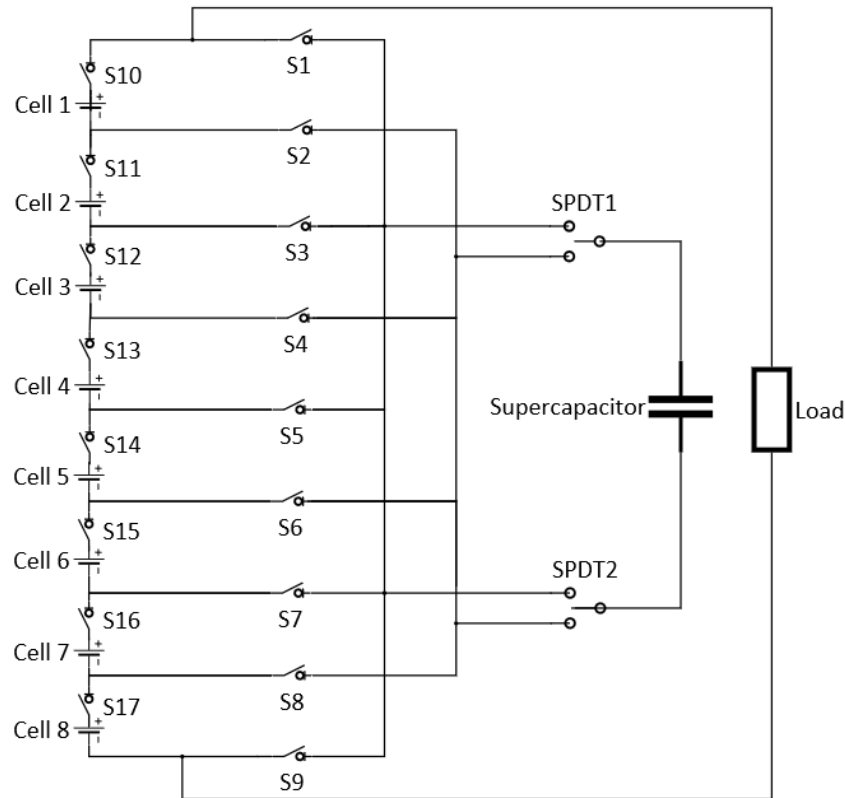


Figure 6.1: New proposed active balancing, balancing circuit

The charged supercapacitor can also be used to charge the lowest SOC cell. For example, cell 2 has the least energy. S2-S3 are turned on, S1 and S4-S9 are turned off, SPDT1 is turned down, and SPDT2 is turned up, which makes the supercapacitor parallel connected to cell 2 and charge it. At the same time, S10-S17 are all turned on, and all cells provide or receive power.

6.2 Balancing Algorithms

During the balancing process, the voltage of the supercapacitor is controlled not to exceed its upper and lower limits. The upper voltage limit is determined by the characteristics of the supercapacitor to avoid it being over-charged. The lower voltage limit is determined by the maximum value of the cell open circle voltage (OCV), ensuring the supercapacitor is capable to charge cells under any SOC.

The flow-chart of balancing algorithms is shown in Figure 6.2. There is a “balancing flag” in the flow-chart which tells whether the supercapacitor is fully charged and ready to deliver energy to other cells. After the battery is powered on, the supercapacitor voltage is first checked. If the voltage is smaller than its upper limit, the “balancing flag” is set to 0 (not ready), otherwise the “balancing flag” is set to 1 (ready).

Requested power of the powertrain system is checked when the “balancing flag” is 0. Positive power means the battery needs to provide traction power and all cells are connected in series to drive the vehicle. Negative power means braking energy is under recovering. SOC levels of all cells are compared and the highest one is found out. The supercapacitor is then connected in cell series and replace the selected one. The “balancing flag” will be changed to 1 when the supercapacitor voltage reaches its upper limit.

When the balancing flag is 1, the supercapacitor will not be further charged and all cells are connected in series. If the maximum SOC difference among all cells is smaller than a threshold, the supercapacitor will not charge any cell. Otherwise, balancing is needed. The selected lowest SOC cell is then parallel connected to and charged by the supercapacitor. When the voltage of the supercapacitor reaches its lower limit, the “balancing flag” is set to 0 again, before starting the next round of the supercapacitor charging and discharging process.

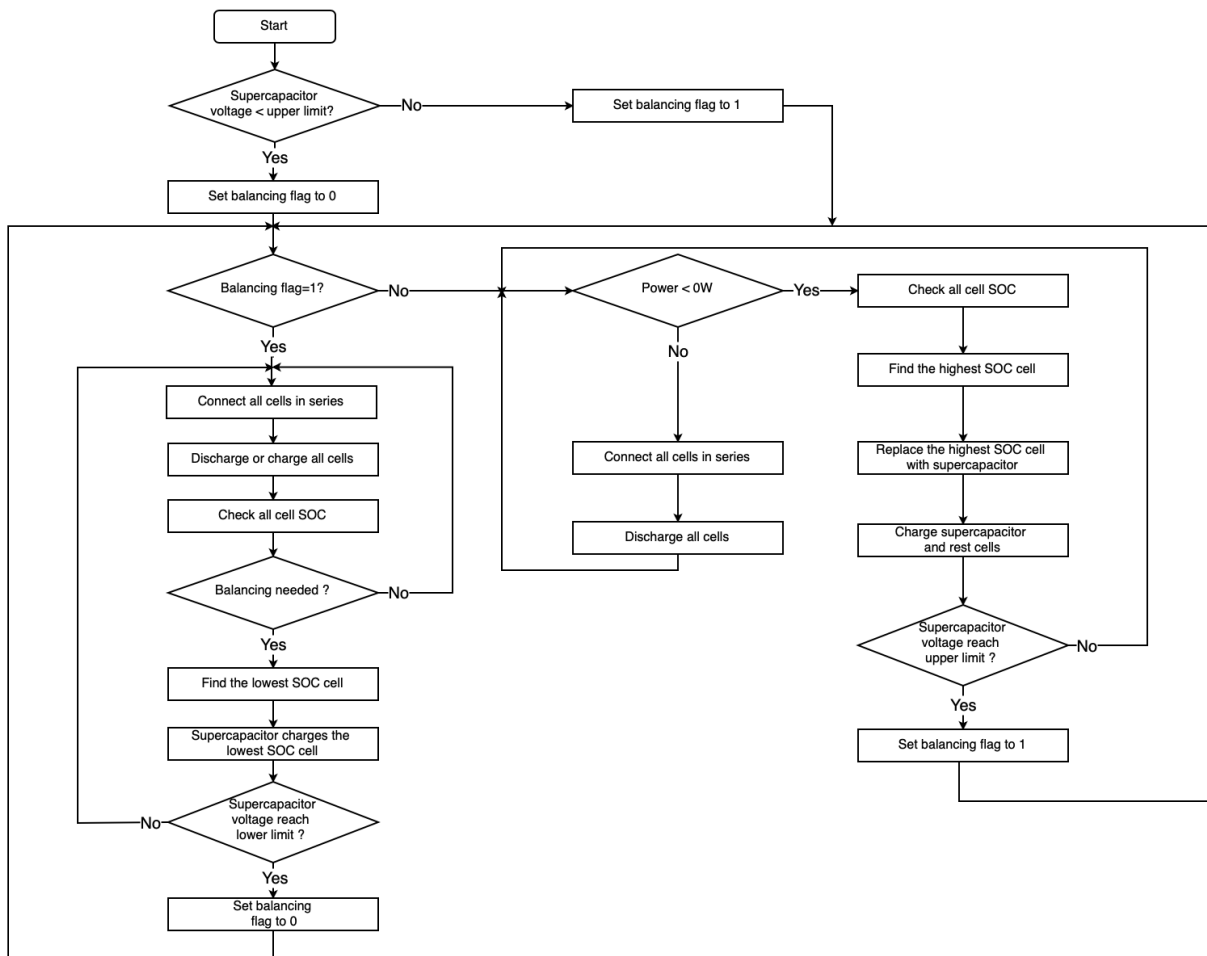


Figure 6.2: New proposed active balancing, flow-chart

6.3 Balancing time calculation

During the complete balancing process, the supercapacitor is repeatedly charged and discharged. The amount of charges (Q_{cycle}) flows into it during one driving cycle is calculated in Equation 6.1.

$$Q_{cycle} = \int_0^{t_{cycle}} \frac{P_g(t)}{U_s + \sum_{i=1}^{n-1} U_{cell_i}} dt \quad (6.1)$$

where t_{cycle} is the time of one driving cycle; P_g is regeneration power; U_s is supercapacitor terminal voltage; n is number of series-connected cells; U_{cell_i} is cell terminal voltage at the i^{th} position after sorting all cells according to their SOC levels.

The supercapacitor and cell terminal voltage change with their energy levels. When doing the calculation, U_s can be simplified to be the average of supercapacitor upper voltage limit ($U_{s,max}$) and lower voltage limit ($U_{s,min}$), and U_{cell} can be simplified to be the cell nominal voltage.

The amount of charges (Q_0) when the supercapacitor is charged from $U_{s,min}$ to $U_{s,max}$ is calculated in Equation 6.2.

$$Q_0 = C_s(U_{s,max} - U_{s,min}) \quad (6.2)$$

where C_s is the supercapacitor capacitance.

The time (t_1) to fully charge the supercapacitor is calculated in Equation 6.3 when repeating driving cycles are used.

$$t_1 = t_{cycle} \frac{Q_0}{Q_{cycle}} \quad (6.3)$$

When the supercapacitor charges one cell, charging current will decrease from I_{s1} to I_{s2} , which are calculated in Equation 6.4 and Equation 6.5.

$$I_{s1} = \frac{U_{s,max} - U_{cell_1}}{r_s + r_{cell_1}} \quad (6.4)$$

$$I_{s2} = \frac{U_{s,min} - U_{cell_1}}{r_s + r_{cell_1}} \quad (6.5)$$

where r_s is ESR of the supercapacitor; U_{cell_1} and r_{cell_1} are terminal voltage and internal resistance of the lowest-SOC cell.

The time (t_2) to discharge the supercapacitor to $U_{s,min}$ is calculated in Equation 6.6, where a linear current change is assumed.

$$t_2 = \frac{2Q_0}{I_{s1} + I_{s2}} \quad (6.6)$$

Before balancing process, the total amount of unbalanced charges (Q_{total}) is calculated in Equation 6.7.

$$Q_{total} = \sum_{i=1}^n (Q_{max} - Q_i) \quad (6.7)$$

where Q_{max} is the maximum amount of charges stored in one cell before balancing; Q_i is the amount of charges stored in any cell before balancing.

After the supercapacitor is charged and discharged one time, $2Q_0$ amount of charges will be balanced. The total time (t_{total}) to balance all cells are calculated in Equation 6.8.

$$t_{total} = (t_1 + t_2) \frac{Q_{total}}{2Q_0} \quad (6.8)$$

Based on the above calculation, the balancing time can be adjusted by selecting different supercapacitor capacitances, upper voltage limits, and lower voltage limits. But these parameters are also limited by supercapacitor self-characteristics and cell voltage.

7 Results and Analysis

7.1 Powertrain Simulation Results

Powertrain models in subsection 2.3 are simulated to check how the reference vehicle driving range can be extended by using battery balancing technologies. Repeating WLTC driving cycles are used for simulation and the battery is discharged until one or several cells reach their lower limit (SOC equals to 0). When there is no balancing, cell initial SOC values are different. When there is passive or active balancing, cell initial SOC values are the same and equal to 1. Cell capacity variation always exists no matter there is balancing or not. Settings of eight cell blocks are according to Figure 7.1.

	Without Balancing		Passive Balancing		Active Balancing	
	Capacity (Ah)	Initial SOC	Capacity (Ah)	Initial SOC	Capacity (Ah)	Initial SOC
Cell 1	25.0	80%	25.0	100%	25.0	100%
Cell 2	22.8	98%	22.8	100%	22.8	100%
Cell 3	23.8	94%	23.8	100%	23.8	100%
Cell 4	24.6	92%	24.6	100%	24.6	100%
Cell 5	24.3	90%	24.3	100%	24.3	100%
Cell 6	24.7	88%	24.7	100%	24.7	100%
Cell 7	24.8	96%	24.8	100%	24.8	100%
Cell 8	22.0	100%	22.0	100%	22.0 </td <td>100%</td>	100%

Figure 7.1: Powertrain simulation, parameter settings

When there is no balancing, simulation results are shown in Figure 7.2. All cells start to be discharged with different initial SOC values but the same discharging power. The SOC of cell 1 firstly reaches 0. At the same time, the discharging process of the battery is stopped even though there is still some energy left in other cells. It should be mentioned that the cell with the lowest initial SOC is not necessarily the one firstly fully discharged since there is still capacity variation among cells which also affects the discharging speed. The vehicle range is calculated by integrating the vehicle speed and equals to 285.4 km.

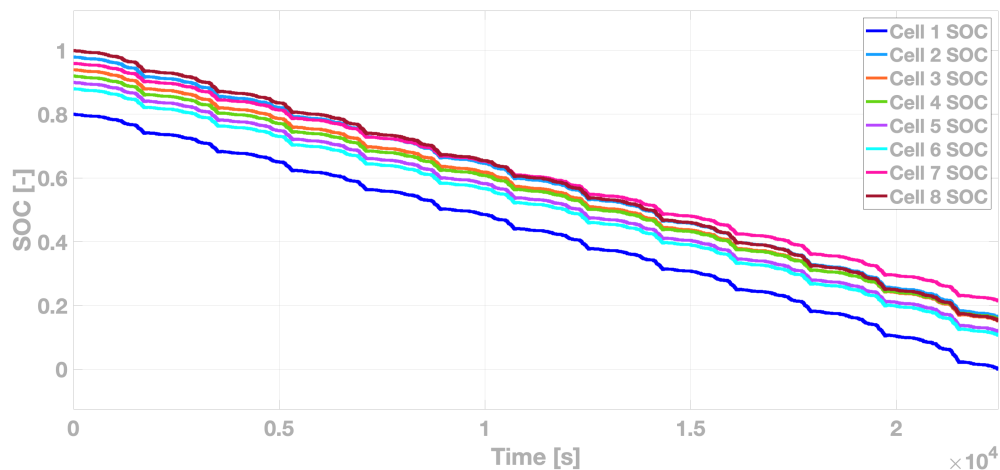


Figure 7.2: Powertrain simulation results, without balancing

As can be seen in Figure 7.3, initial SOC values of all cells equal to 1 when there is passive balancing in the battery. Since there is capacity variation among cells, the cell SOC decreasing speeds are different even though all cells provide an identical amount of power. Cell 1 has the smallest capacity which makes it be fully discharged firstly. As a result, energy in the other seven cells can not be totally used. Because more energy is saved in the battery before the discharging process thanks to the passive balancing, the vehicle range is extended to 322.2 km.

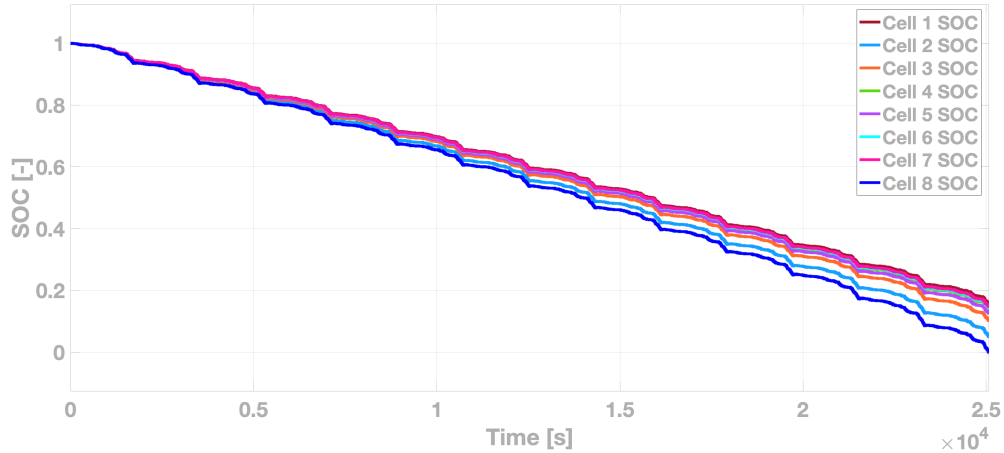


Figure 7.3: Powertrain simulation results, with passive balancing

When active balancing is used, simulation results are shown in Figure 7.4. It can be found that eight cells are fully charged and discharged at the same time, which means all available battery energy is used. Because of the active balancing, cells can be discharged with controlled different powers to maintain the biggest SOC difference is always smaller than 0.1%. The vehicle range is the biggest when the active balancing is used in the battery, which is 353.8 km.

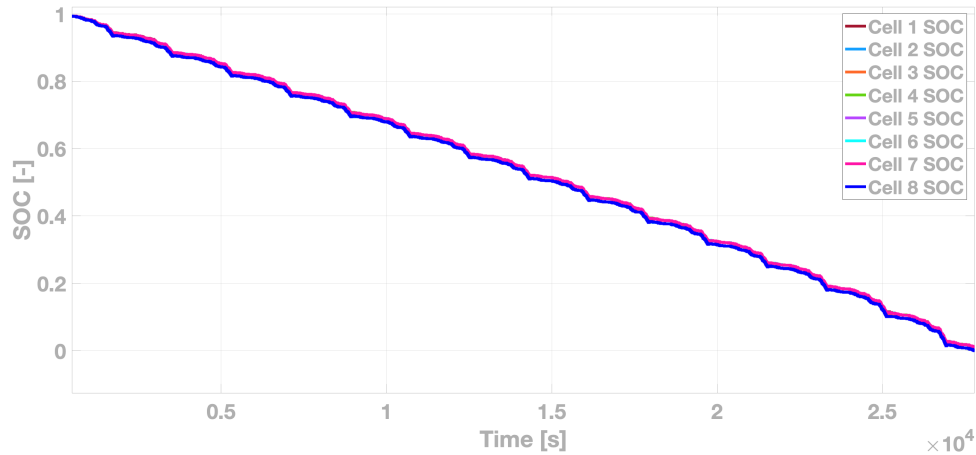


Figure 7.4: Powertrain simulation results, with active balancing

Based on the above analysis, it can be concluded that the active balancing is better than the passive balancing and better than without balancing, regarding the vehicle range when the same group of cells and driving cycle are used. Balancing technologies are capable to improve battery energy utilization, although more control algorithms are needed. To make the simulation results more visually intuitive, a bar chart of vehicle ranges is drowned in Figure 7.5.

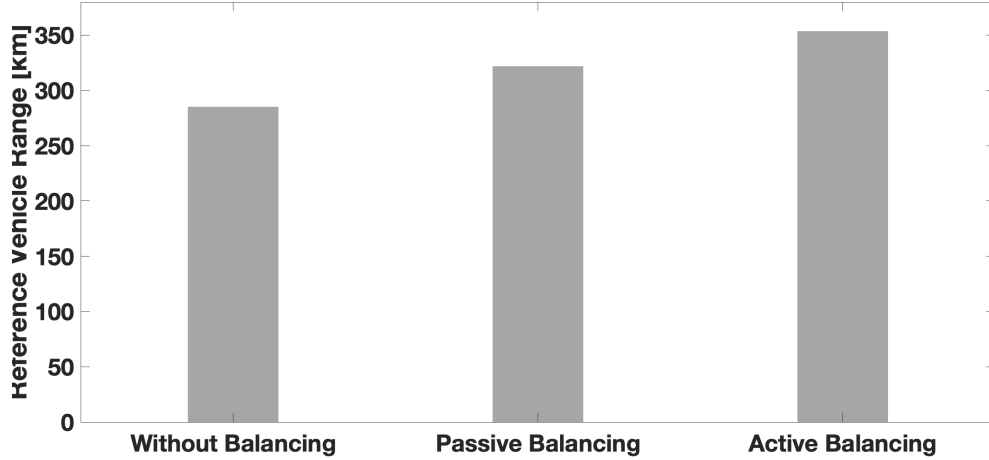


Figure 7.5: Powertrain simulation results, reference vehicle range compare

7.2 Passive Balancing Simulation Results

The *switched resistor balancing* model introduced in subsection 4.2 is simulated. The parameters in eight cell blocks are set according to Figure 7.6 to simulate SOC and capacity variations.

	Cell 1	Cell 2	Cell 3	Cell 4	Cell 5	Cell 6	Cell 7	Cell 8
Capacity (Ah)	23.8	23.5	23.6	24.1	24.3	24.2	23.9	24.5
Initial SOC	24.37%	21.28%	19.49%	19.09%	17.70%	15.29%	12.13%	12.24%

Figure 7.6: Switched resistor balancing simulation, parameter settings

After the charging process is started, all cells are charged with 24 A until the SOC of cell 1 reaches its upper limit at 2700s. This is also the time when passive balancing is activated in the battery. The SOC curve of cell 1 is shown in Figure 7.7. It can be found that cell 1 is discharged and charged repeatedly during the balancing process, and its SOC can be kept fluctuating between 0.98 and 1 to avoid overcharging.

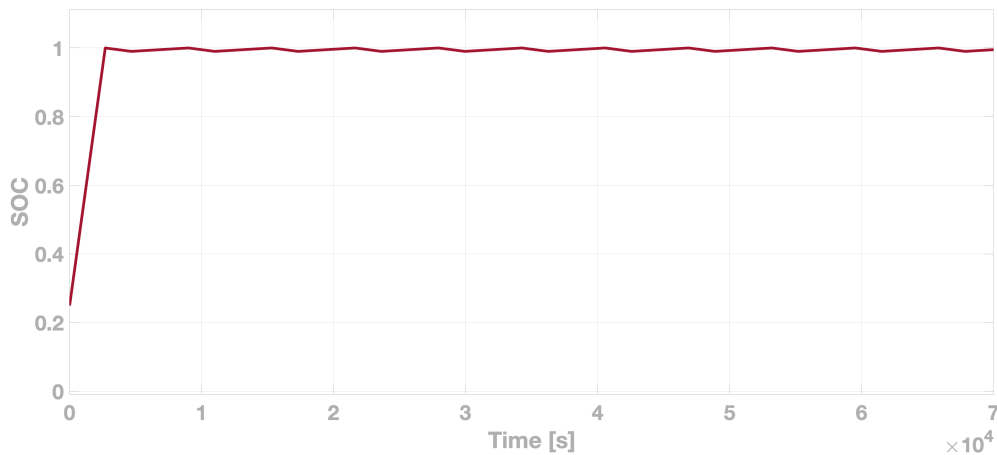


Figure 7.7: Switched resistor balancing simulation results, cell 1 SOC curve

Balancing current passing through the shunt resistor of cell 1 is drawn in Figure 7.8. It can be found that the balancing current is 0 A at the beginning since no balancing is needed. At 2700s, there is 0.65 A current passing through the shunt resistor to dissipate exceeded energy in cell 1. At 4678s, cell 1 is discharged to 0.98 SOC and the balancing current is set to 0 A again by controlling the corresponding switch. Afterward, cell 1 is charged with 0.2 A for another 4320s before its SOC reaches 1 again. The balancing current is thus changing periodically, which also aligns with the SOC curve of cell 1.

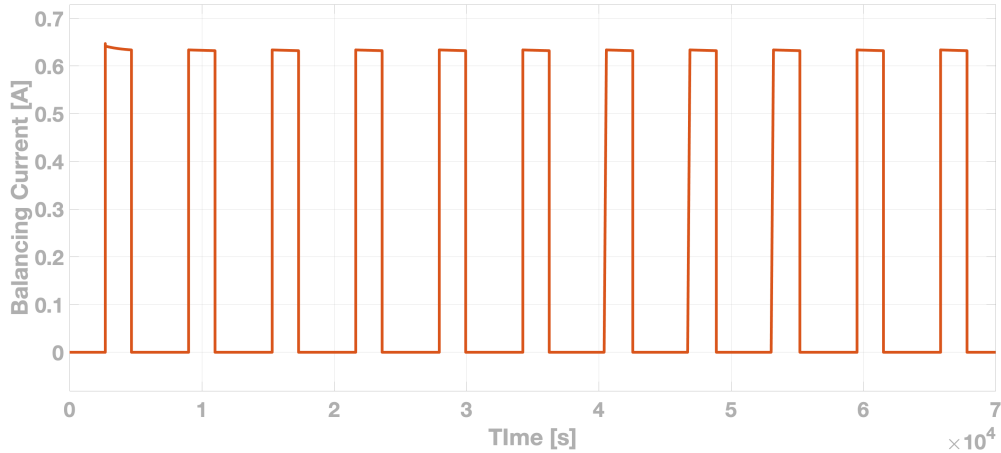


Figure 7.8: Switched resistor balancing simulation results, balancing current

SOC curves of eight cells are drawn in one figure, which is shown in Figure 7.9. It can be found that their initial SOC values before the charging process are different. And slopes of different SOC lines are also different even though all cells are charged with the same current at the beginning. This is caused by the different capacities of eight cells, which makes SOC increasing speeds also different. After cell 1 starts to be balanced at 2700s, the other cells are also set into balancing modes once their SOC values reach 1. Cell 8 is the last one to be fully charged at 65840s, when battery charging and balancing process is finished.

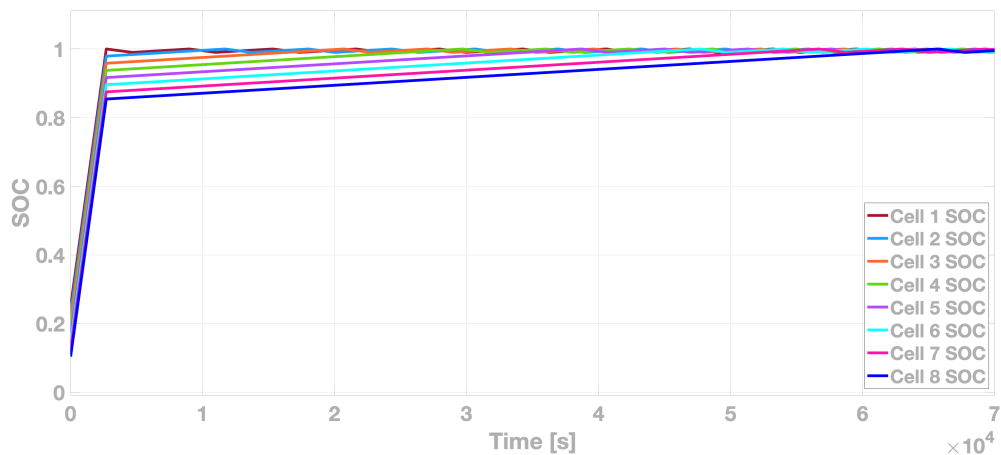


Figure 7.9: Switched resistor balancing simulation results, balancing curve

It should be mentioned that the constant current mode can charge the battery very fast. Only 45 minutes are needed to charge the battery from around 0.2 SOC to 0.9 SOC at the beginning. However, once one cell is fully charged the charging speed is largely reduced, and the constant-voltage mode can only use a very small charging current. It takes more than 17 hours to charge the last 10% of battery energy and realize balancing among eight cells.

7.3 Active Balancing Simulation Results

7.3.1 Single Switched-Capacitor Balancing Simulation Results

The *single switched-capacitor balancing* introduced in subsection 5.4.1 is simulated. Since the simulation speed is rather slow in active balancing models, SOC variation is set to be smaller than that in the passive balancing model, which is shown in Figure 7.10.

	Cell 1	Cell 2	Cell 3	Cell 4	Cell 5	Cell 6	Cell 7	Cell 8
Capacity (Ah)	23.8	23.5	23.6	24.1	24.3	24.2	23.9	24.5
Initial SOC	97.69%	97.45%	98.73%	98.96%	98.35%	98.55%	98.66%	98.16%

Figure 7.10: Single switched-capacitor balancing simulation, parameter settings

Cell 4 has the biggest initial SOC, and its SOC curve is shown in Figure 7.11. It can be found that the slope of this curve is in most time negative, but sometimes it is also positive. This is caused by the regeneration process of the powertrain system and the battery is charged when the vehicle is decelerated. This SOC curve also aligns with the module power curve shown in Figure 3.5.

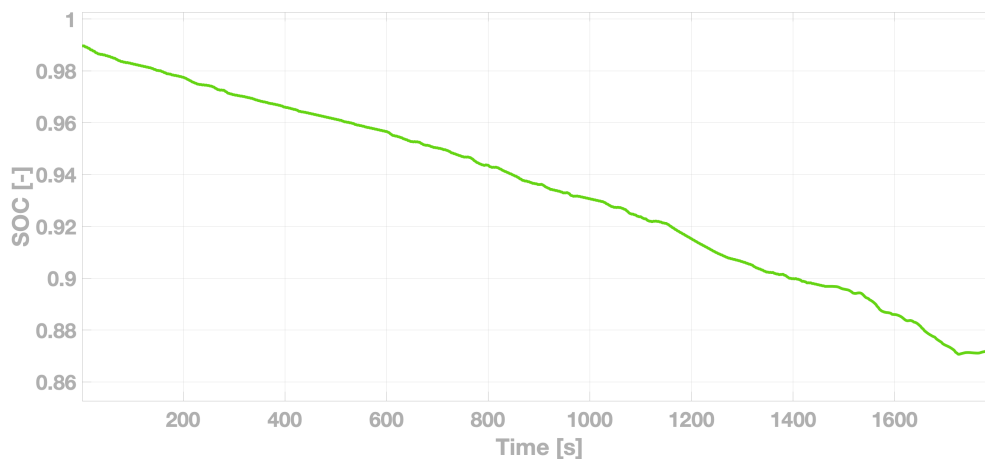


Figure 7.11: Single switched-capacitor balancing simulation results, cell 4 SOC curve

Balancing current passing through the capacitor is shown in Figure 7.12. Every 5 seconds is one balancing cycle. During the first 2.5 seconds, the capacitor is charged by the complete module, and the capacitor current is positive. During the second 2.5 seconds, the capacitor is discharged by the lowest SOC cell which makes its current negative. Before 220s, we can find that absolute values of capacitor charging currents are bigger than discharging currents. This is because more charges need to be stored in the capacitor to build up the capacitor voltage. After 220s, the balancing current is stabilized by fluctuating between around +7A and -7A. This means the same amount of charges is delivered in and delivered out the capacitor in every balancing cycle, and the capacitor voltage also steadily fluctuates. By taking a detailed observation, the absolute values of the balancing current have little variation with time. The reason is that the complete module and the selected cell voltages are both changing during the simulation. Firstly, the module is discharged and its voltage changes with SOC of each cell. Secondly, the position of the lowest SOC cell also changes, which brings an inconstant cell voltage. At about 1480s, the balancing process is first time stopped and the balancing current is set to 0 A. If the SOC difference is found to be bigger than 0.1% afterward, the balancing process will be activated again immediately.

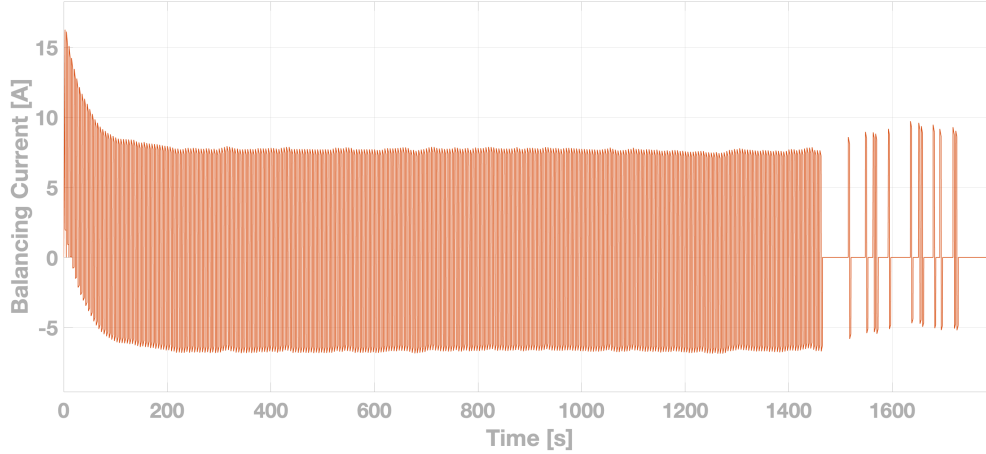


Figure 7.12: Single switched capacitor balancing simulation results, balancing current

The balancing curve is shown in Figure 7.13. In the beginning, cell 2 is the lowest SOC cell. The complete module charges the capacitor, and the capacitor charges cell 2 only. The other seven cells have the same SOC curve slope at the beginning. At about 120s, the cell 2 and cell 1 SOC curves intersect. These two cells are then alternatively charged by the capacitor. More and more cell SOC curves coincide afterward. At about 1480s, eight cells are first time balanced when the maximum SOC difference is smaller than 0.1%.

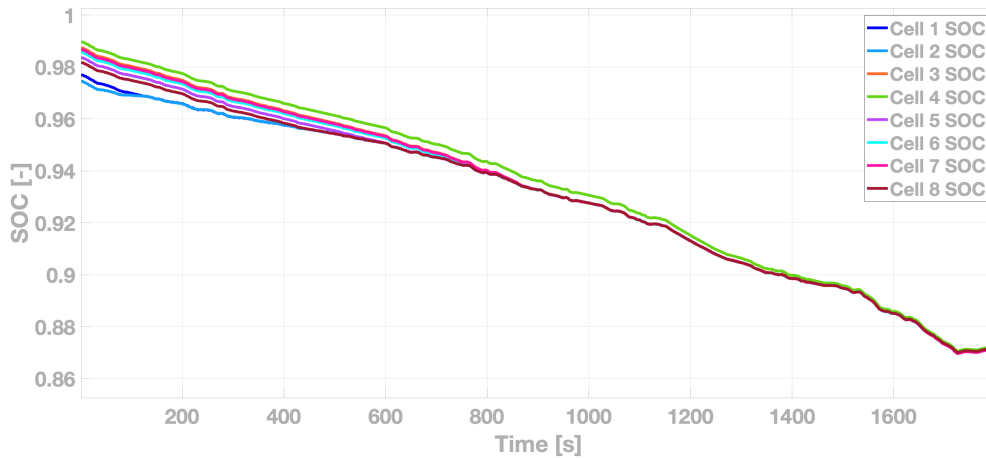


Figure 7.13: Single switched capacitor balancing simulation results, balancing curve

7.3.2 Multi Inductor Balancing Simulation Results

The *multi inductor balancing* model is simulated with the same cell capacity and initial SOC settings as shown in Figure 7.10. It can be found that the SOC difference between cell 2 and cell 3 is the biggest at the beginning, and these two cells are firstly balanced by the second inductor. The balancing current passing through this inductor is shown in Figure 7.14. Within one balancing cycle, the inductor is firstly charged by cell 3 until its current reaches 30A. Afterward, the inductor is discharged to deliver its energy to cell 2 until its current becomes 0 A. Because of the current-based closed-loop control algorithms, balancing current always exists in one of seven inductors if the balancing is needed, which reduces the required balancing time compared to the discontinuous conduction mode (DCM). It can also be found that the period of every balancing cycle is not a constant value. Switching frequencies are changing with inductor current slopes which are determined by the balanced cell voltages.

The balancing curve is shown in Figure 7.15. Cell 2 and cell 3 are firstly balanced with their SOC lines becoming closer and closer to each other. The other six cells are discharged evenly in the beginning. After

about 36.6s, the cell couple (cell 2 and cell 3) and the cell couple (cell 3 and cell 4) start to be alternatively balanced. During the balancing process, only one couple of cells can be balanced at the same time, and the balancing is finally achieved at about 502s when the maximum SOC difference is smaller than 0.1%.

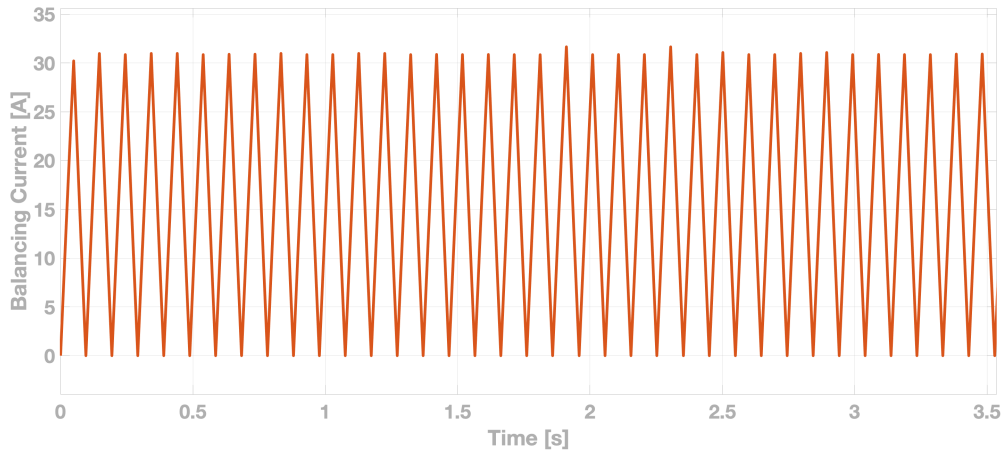


Figure 7.14: Multi inductor balancing simulation results, balancing current

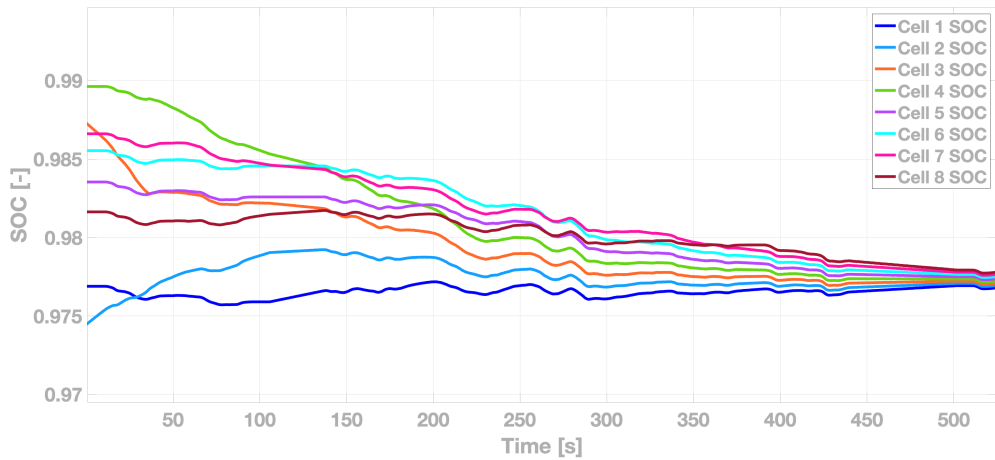


Figure 7.15: Multi inductor balancing simulation results, balancing curve

7.3.3 Buck Boost Converter Balancing Simulation Results

Due to the slow simulation speed of the *buck boost converter balancing* model, cell nominal capacity is scaled down to 24mA. But cell capacity and initial SOC variation are kept at the same level (Figure 7.16). Since the required balancing time is also scaled down and becomes less than one second, the WLTC driving cycle (1800s) is not used in this simulation, and constant power is used to discharge the battery.

	Cell 1	Cell 2	Cell 3	Cell 4	Cell 5	Cell 6	Cell 7	Cell 8
Capacity (mAh)	23.8	23.5	23.6	24.1	24.3	24.2	23.9	24.5
Initial SOC	97.69%	97.45%	98.73%	98.96%	98.35%	98.55%	98.66%	98.16%

Figure 7.16: Buck boost converter balancing simulation, parameter settings

The balancing curve is shown in Figure 7.17. It can be found that cell 4 is the highest SOC cell at the beginning and it is also discharged fastest. Cell 2 is the lowest SOC cell whose SOC curve slope is the smallest at first. All the other six cells are discharged under the same middle speed. At about 0.052s, SOC curves of cell 4 and cell 3 intersect, and these two cells alternatively have the biggest voltage conversion ratio and the biggest discharging power. Similarly, at about 0.22s, cell 2 and cell 1 also alternatively become the lowest SOC cell and be discharged slowest. At about 0.71s, eight cells are all balanced with the SOC difference smaller than 0.1%.

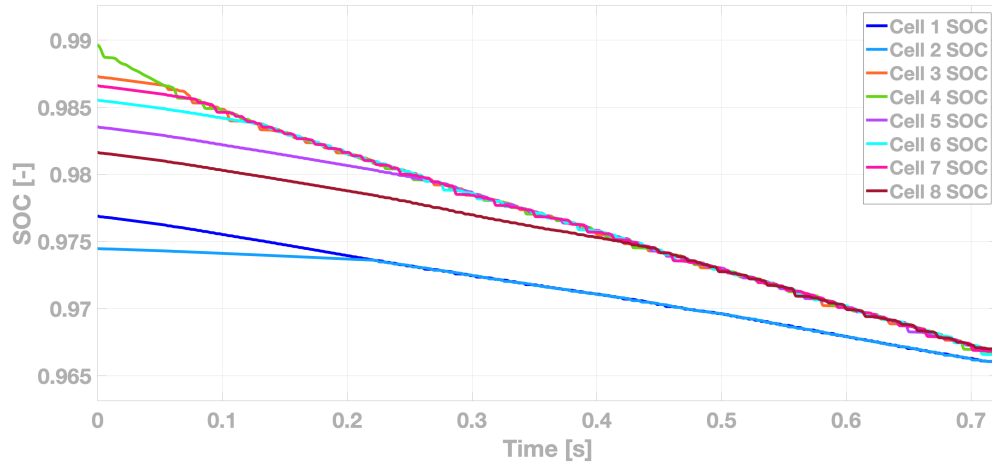


Figure 7.17: Buck boost converter balancing simulation results, balancing curve

Output voltages of buck boost converters and the complete module are shown in Figure 7.18. The output voltages of the buck boost converters are proportionally related to cell SOC. The module output voltage is maintained at about 35V. It should be mentioned that this voltage curve is drawn when normal size cells (24Ah) are used and longer balancing time is needed.

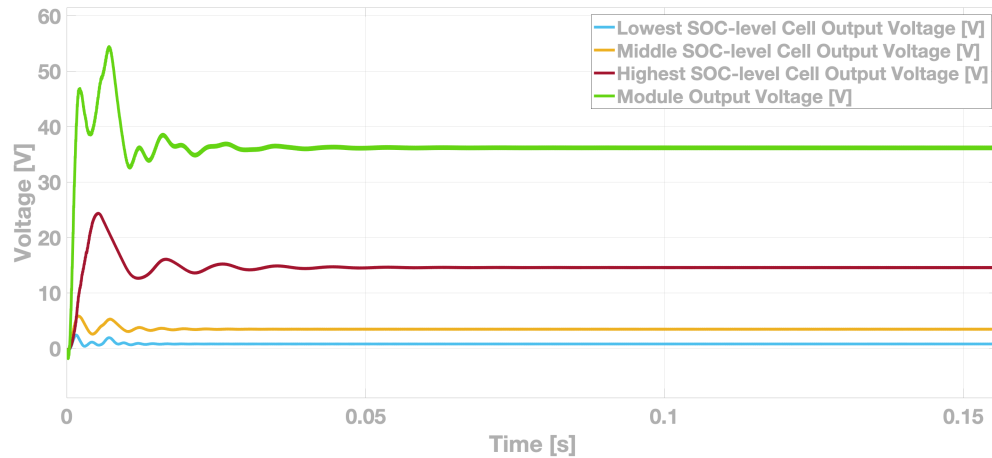


Figure 7.18: Buck boost converter balancing simulation results, cell and module voltage

7.4 New Proposed Active Balancing Simulation Results

The new proposed active balancing method is also simulated. Different cell capacities and initial SOC are shown in Figure 7.19. Since the SOC variation is bigger in this simulation, WLTC driving cycle is repeatedly used until all cells are balanced.

	Cell 1	Cell 2	Cell 3	Cell 4	Cell 5	Cell 6	Cell 7	Cell 8
Capacity (Ah)	23.8	23.5	23.6	24.1	24.3	24.2	23.9	24.5
Initial SOC	74.00%	72.50%	73.00%	75.00%	71.50%	74.50%	73.50%	72.00%

Figure 7.19: New proposed active balancing simulation, parameter settings

The currents passing through the supercapacitor, cell 4, and cell 5 are shown in Figure 7.21 and Figure 7.20. The balancing curve is shown in Figure 7.22.

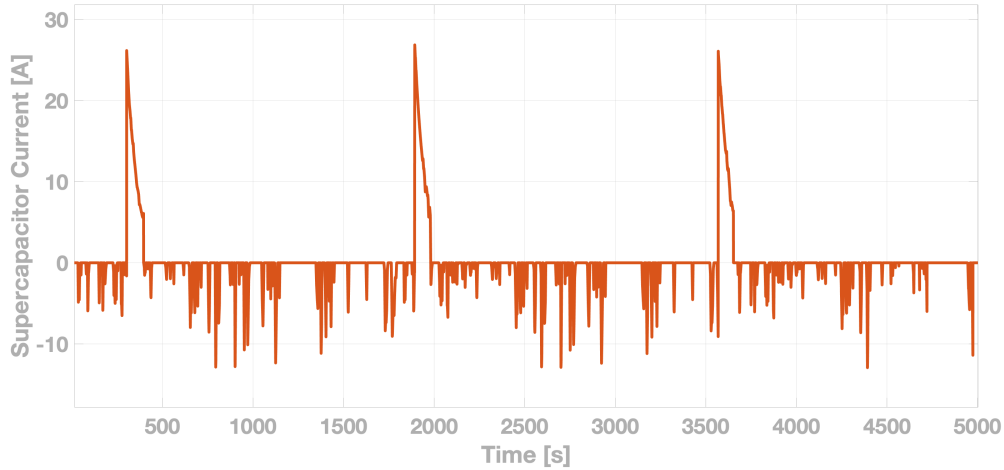


Figure 7.20: New proposed active balancing simulation results, supercapacitor current

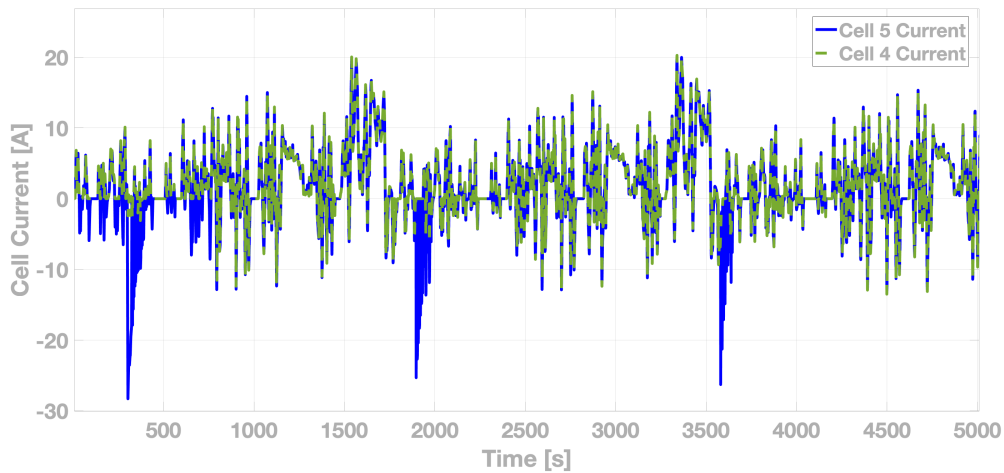


Figure 7.21: New proposed active balancing simulation results, cell 4 and cell 5 current

In the beginning, cell 4 has the biggest SOC, and it is not charged during the regeneration process. Therefore, charging current of cell 4 is 0 A, and its SOC decreases faster than the others. The supercapacitor has charging current at the start until it is charged to its upper voltage limit at 302s. Afterward, the energy in the supercapacitor flows into the lowest SOC cell (cell 5). Accordingly, the cell 5 has bigger charging current while the supercapacitor has discharging current. At 322s, cell 5 and cell 8 both become the lowest

SOC cells and they start to be alternatively charged. At 396s, the supercapacitor is the first time discharged to its lower voltage limit and its current is changed back to charging. It should be mentioned that during the discharging process of the supercapacitor, cell 4 is able to be charged by regeneration power and has charging current, although it is still the highest SOC cell. After about three times of charging and discharging the supercapacitor, eight cells are finally balanced at 4390s when the SOC difference is smaller than 0.1%.

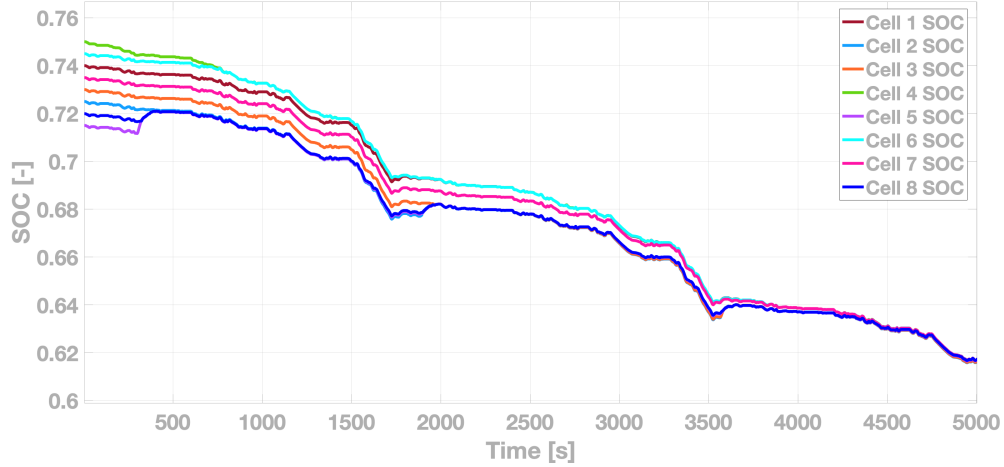


Figure 7.22: New proposed active balancing simulation results, balancing curve

The *single switched-capacitor balancing* is simulated with the same settings as shown in Figure 7.19. The balancing curve in Figure 7.23 shows it takes 4700s to balance all cells, which is slower than the proposed one. If the driving cycle is changed to congested city road conditions when more braking is needed, the balancing speed of the proposed one will be even faster.

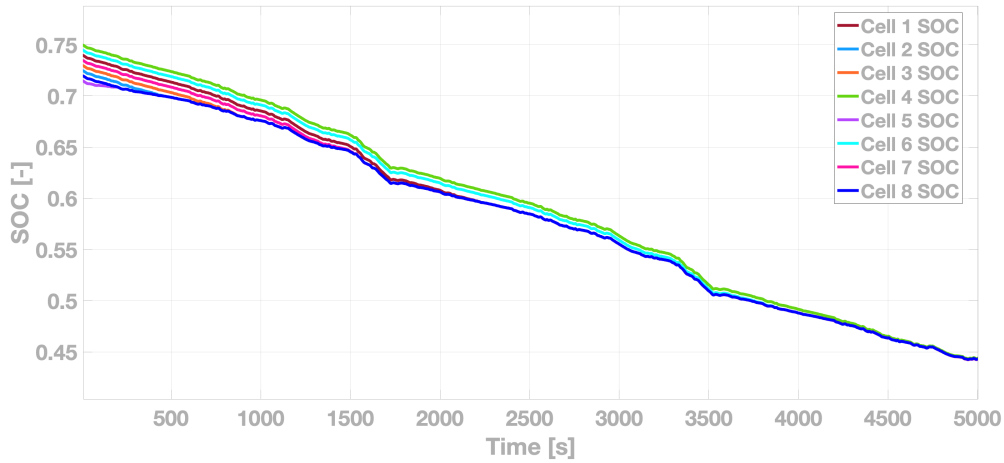


Figure 7.23: Single switched-capacitor balancing simulation results, balancing curve

8 Conclusions

8.1 Conclusions

Based on literature reviews, battery balancing technologies have two big categories, passive balancing and active balancing, based on whether exceeded energy is dissipated in the form of heat. The active balancing methods have three main groups: capacitor based balancing, inductor based balancing, converter based balancing. Capacitor based active balancing methods generally have long balancing time, but additional structures can be added to provide more charge-transfer paths and improve balancing speed. Inductor based active balancing methods have bigger balancing current and shorter balancing time, but switch losses are also higher. Converter based active balancing methods actively control cell output power or transfer charges among cells, and they have good control flexibility but also need more components and add more costs. A summary sheet is given to compare most existing battery balancing technologies from different perspectives.

24Ah Lithium-ion pouch cells are used in this thesis work. A battery configuration with ninety-six cells in series and six cells in parallel can meet the reference vehicle requirements. The battery is scaled down for full-electric powertrain modeling. Powertrain simulation results show that passive balancing can increase the reference vehicle range from 285.4 km to 322.2 km compared to no balancing, when the maximum SOC difference is 20%. Active balancing can further improve the vehicle range to 353.8 km since all cells are fully charged and discharged at the same time and utilized battery energy is also the most.

Battery models with different balancing methods are built, which uses 2-RC equivalent circuit model for Lithium-ion cell modeling. The *switched resistor balancing* has the longest balancing time, and the balancing current shall offset the low-speed charging current to avoid cell over-charging happening. By transferring charges between the complete module and the lowest SOC cell in the *single switched-capacitor balancing*, the balancing speed is faster due to the bigger voltage difference. Close-loop control of the balancing current in the *multi inductor balancing* can fully use the time to balance adjacent cells. In the *buck boost converter balancing*, voltage conversion ratios of converters shall be set not only to balance cells but also to maintain a stable module output voltage.

The proposed active balancing method with one supercapacitor can balance eight series-connected cells in 4390s with maximum initial SOC difference as 3.5% and under the WLTC driving cycle, which is faster compared to the *single switched-capacitor balancing*. The proposed method uses the supercapacitor to replace the highest SOC cell during the vehicle regeneration process, reducing times of energy conversion and improving battery overall efficiency.

8.2 Future Work

The balancing performance of the proposed active balancing method has been validated by Simulink simulations, but the improvement of battery efficiency by utilizing this new topology needs further confirmed with more experiments. What's more, the functions of this topology can be further developed when battery thermal performance and cell state of health (SOH) are taken into consideration. Besides balancing SOC of cells, the supercapacitor can also be used as an additional energy source to provide traction power and reduce the working time of low SOH cells or high temperature cells, increasing the amount of battery usable energy as well as extending the battery lifetime.

References

- [1] J. Wu, A. Emadi, M. J. Duoba, and T. P. Bohn, "Plug-in hybrid electric vehicles: Testing, simulations, and analysis," pp. 469–476, 2007.
- [2] J. G. Bruno Scrosati, "Lithium batteries: Status, prospects and future," *Journal of Power Sources*, vol. 195, no. 9, pp. 2419–2430, 2010.
- [3] B. T. Kuhn, G. E. Pitel, and P. T. Krein, "Electrical properties and equalization of lithium-ion cells in automotive applications," pp. 5 pp.–, 2005.
- [4] L. P. C. Z. B. X. Xiaoyu Li, Tiansi Wang, "A comparative study of sorting methods for lithium-ion batteries," *2014 IEEE Conference and Expo Transportation Electrification Asia-Pacific*, 2014.
- [5] H. K. C. Y. A. P. Dafen Chen, Jiuchun Jiang, "Comparison of different cooling methods for lithium ion battery cells," *Journal of Applied Thermal Engineering*, vol. 94, pp. 846–854, 2016.
- [6] H. J. N. Maleki Hossein, "Effects of overdischarge on performance and thermal stability of a li-ion cell," *Journal of Power Sources*, vol. 160, pp. 1395–1402, 2006.
- [7] R. W. B. N. P. Ramadass, BalaHaran, "Performance study of commercial licoo2 and spinel-based li-ion cells," *Journal of Power Sources*, vol. 111, pp. 210–220, 2002.
- [8] L. Wei, L. Jie, S. Wenji, and F. Ziping, "Study on passive balancing characteristics of serially connected lithium-ion battery string," pp. 489–495, 2017.
- [9] D. C. C. Lucian Andrei Perișoară, Ionuț Constantin Guran, "A passive battery management system for fast balancing of four lifepo4 cells," *2018 IEEE 24th International Symposium for Design and Technology in Electronic Packaging*, 2018.
- [10] M. I. M.-M. M. A. G.-M. Javier Gallardo-Lozano, Enrique Romero-Cadaval, "Battery equalization active methods," *Journal of Power Sources*, vol. 246, pp. 934–949, 2014.
- [11] M. Caspar, T. Eiler, and S. Hohmann, "Systematic comparison of active balancing: A model-based quantitative analysis," *IEEE Transactions on Vehicular Technology*, vol. 67, no. 2, pp. 920–934, 2018.
- [12] B. Jacobson, *Chalmers vehicle dynamics compendium*. Chalmers, 2018.
- [13] R. Barnard, *Road vehicle aerodynamic design : an introduction*. Gardners Books, 2009.
- [14] https://en.wikipedia.org/wiki/Tesla_Model_3 Accessed April 4, 2020.
- [15] https://en.wikipedia.org/wiki/Worldwide_Harmonised_Light_Vehicles_Test_Procedure Accessed April 4, 2020.
- [16] L. Guzzella and A. Amstutz, "Cae tools for quasi-static modeling and optimization of hybrid power-trains," *IEEE Transactions on Vehicular Technology*, vol. 48, no. 6, pp. 1762–1769, 1999.
- [17] E. T. H. Zürich, *The QSS Toolbox Manual*, 2005.
- [18] H. Berg, *Batteries for electric vehicles: Materials and electrochemistry*. Cambridge University Press, 2015.
- [19] J. M. Aden Seaman, Thanh-Son Dao, "A survey of mathematics-based equivalent-circuit and electro-chemical battery models for hybrid and electric vehicle simulation," *Journal of Power Sources*, 2014.
- [20] R. Gu, P. Malysz, H. Yang, and A. Emadi, "On the suitability of electrochemical-based modeling for lithium-ion batteries," *IEEE Transactions on Transportation Electrification*, vol. 2, no. 4, pp. 417–431, 2016.

- [21] S. D. S. S. R. D. B.-V. R. S. Venkatasailanathan Ramadesigan, Paul W. C. Northrop, "Modeling and simulation of lithium-ion batteries from a systems engineering perspective," *Journal of The Electrochemical Society*, 2012.
- [22] P. J. S. Stephen W. Moore, "A review of cell equalization methods for lithium ion and lithium polymer battery systems," *SAE 2001 World Congress*, 2001.
- [23] N. H. Kutkut and D. M. Divan, "Dynamic equalization techniques for series battery stacks," pp. 514–521, 1996.
- [24] M. Daowd, N. Omar, P. Van Den Bossche, and J. Van Mierlo, "Passive and active battery balancing comparison based on matlab simulation," pp. 1–7, 2011.
- [25] A. N. A. N. Amin, Kristian Ismail, "Passive balancing battery management system using mosfet internal resistance as balancing resistor," *2017 International Conference on Sustainable Energy Engineering and Application*, 2017.
- [26] L. Wei, L. Jie, S. Wenji, and F. Ziping, "Study on passive balancing characteristics of serially connected lithium-ion battery string," pp. 489–495, 2017.
- [27] J. Qi and D. Dah-Chuan Lu, "Review of battery cell balancing techniques," pp. 1–6, 2014.
- [28] J. C. Jonathan Carter, Zhong Fan, "Cell equalisation circuits: A review," *Journal of Power Sources*, vol. 448, 2020.
- [29] C. Pascual and P. T. Krein, "Switched capacitor system for automatic series battery equalization," vol. 2, pp. 848–854 vol.2, 1997.
- [30] A. Baughman and M. Ferdowsi, "Double-tiered capacitive shuttling method for balancing series-connected batteries," pp. 109–113, 2005.
- [31] Y. Takeda and H. Koizumi, "Modularized double-tiered switched capacitor voltage equalizer," pp. 2782–2787, 2017.
- [32] M. Kim, C. Kim, J. Kim, and G. Moon, "A chain structure of switched capacitor for improved cell balancing speed of lithium-ion batteries," *IEEE Transactions on Industrial Electronics*, vol. 61, no. 8, pp. 3989–3999, 2014.
- [33] Y. Ye, K. W. E. Cheng, Y. C. Fong, X. Xue, and J. Lin, "Topology, modeling, and design of switched-capacitor-based cell balancing systems and their balancing exploration," *IEEE Transactions on Power Electronics*, vol. 32, no. 6, pp. 4444–4454, 2017.
- [34] Y. Ye and K. W. E. Cheng, "Modeling and analysis of series-parallel switched-capacitor voltage equalizer for battery/supercapacitor strings," *IEEE Journal of Emerging and Selected Topics in Power Electronics*, vol. 3, no. 4, pp. 977–983, 2015.
- [35] Y. Shang, C. Zhang, N. Cui, and C. C. Mi, "A delta-structured switched-capacitor equalizer for series-connected battery strings," *IEEE Transactions on Power Electronics*, vol. 34, no. 1, pp. 452–461, 2019.
- [36] Y. Shang, Q. Zhang, N. Cui, B. Duan, and C. Zhang, "An optimized mesh-structured switched-capacitor equalizer for lithium-ion battery strings," *IEEE Transactions on Transportation Electrification*, vol. 5, no. 1, pp. 252–261, 2019.
- [37] R. Fukui and H. Koizumi, "Double-tiered switched capacitor battery charge equalizer with chain structure," pp. 6715–6720, 2013.
- [38] K.-B. P. G.-W. M. J.-H. L. Hong-Sun Park, Chol-Ho Kim, "Design of a charge equalizer based on battery modularization," *IEEE Transactions on Vehicular Technology*, 2009.
- [39] Y. Takeda and H. Koizumi, "Modularized double-tiered switched capacitor voltage equalizer," pp. 2782–2787, 2017.

- [40] N. O. P. L. P. V. D. B. J. V. M. Mohamed Daowd, Mailier Antoine, “Battery management system—balancing modularization based on a single switched capacitor and bi-directional dc/dc converter with the auxiliary battery,” 2014.
- [41] T. H. Phung, J. Crebier, A. Chureau, A. Collet, and V. Nguyen, “Optimized structure for next-to-next balancing of series-connected lithium-ion cells,” pp. 1374–1381, 2011.
- [42] C. Hua, Y. Fang, and J. Huang, “Inductor based equalizer with a chain structure of switched capacitor to improve balancing speed,” pp. 2151–2154, 2015.
- [43] A. F. Moghaddam and A. Van Den Bossche, “An active cell equalization technique for lithium ion batteries based on inductor balancing,” pp. 274–278, 2018.
- [44] S. Park, Tae-Sung Kim, Jin-Sik Park, Gun-Woo Moon, and Myung-Joong Yoon, “A new battery equalizer based on buck-boost topology,” pp. 962–965, 2007.
- [45] H. Liu and C. Xia, “An efficient battery balancing scheme in electric vehicle,” vol. 2, pp. 541–544, 2013.
- [46] L. Yu, Y. Hsieh, W. Liu, and C. Moo, “Balanced discharging for serial battery power modules with boost converters,” pp. 449–453, 2013.
- [47] C.-H. H. Tsung-Hsi Wu, Chin-Sien Moo, “A battery power bank with series-connected buck–boost-type battery power modules,” 2017.
- [48] R. Koch, A. Jossen, and R. Kuhn, “Novel bidirectional multiple-input multiple-output converter for simultaneous direct battery module balancing,” pp. 1–7, 2013.
- [49] D. G. ELVIRA, H. VALDERRAMA BLAVÍ, J. M. BOSQUE MONCUSÍ, CID PASTOR, J. A. GARRIGA CASTILLO, and L. MARTÍNEZ SALAMERO, “Active battery balancing via a switched dc/dc converter: Description and performance analysis,” pp. 1–6, 2019.
- [50] Z. Nie and C. Mi, “Fast battery equalization with isolated bidirectional dc-dc converter for phev applications,” pp. 78–81, 2009.
- [51] Yuang-Shung Lee, Chun-Yi Duh, Guo-Tian Chen, and Shen-Ching Yang, “Battery equalization using bi-directional cuk converter in dcvm operation,” pp. 765–771, 2005.
- [52] A. F. Moghaddam and A. Van den Bossche, “A battery equalization technique based on Ćuk converter balancing for lithium ion batteries,” pp. 1–4, 2019.
- [53] Y. Lee, C. Tsai, Y. Ko, and M. Cheng, “Charge equalization using quasi-resonant converters in battery string for medical power operated vehicle application,” pp. 2722–2728, 2010.
- [54] Y. . Lee and G. . Cheng, “Quasi-resonant zero-current-switching bidirectional converter for battery equalization applications,” *IEEE Transactions on Power Electronics*, vol. 21, no. 5, pp. 1213–1224, 2006.
- [55] J. Shin, G. Seo, C. Chun, and B. Cho, “Selective flyback balancing circuit with improved balancing speed for series connected lithium-ion batteries,” pp. 1180–1184, 2010.
- [56] C.-E. K. J.-H. L. Chol-Ho Kim, Hong-Sun Park, “Individual charge equalization converter with parallel primary winding of transformer for series connected lithium-ion battery strings in an hev,” *Journal of power electronics*, 2009.
- [57] Feng Ran, Hao Xu, Yuan Ji, Jiaqi Qin, and Wenhui Li, “An active balancing circuit for lithium battery management system with optoelectronic switches,” pp. 1–5, 2015.
- [58] C. Bonfiglio and W. Roessler, “A cost optimized battery management system with active cell balancing for lithium ion battery stacks,” pp. 304–309, 2009.

- [59] A. Farzan Moghaddam and A. Van den Bossche, “Flyback converter balancing technique for lithium based batteries,” pp. 1–4, 2019.
- [60] C. Speltino, A. Stefanopoulou, and G. Fiengo, “Cell equalization in battery stacks through state of charge estimation polling,” pp. 5050–5055, 2010.
- [61] L. L. X. H. M. O. Dongsheng Ren, Xuning Feng, “Overcharge behaviors and failure mechanism of lithium-ion batteries under different test conditions,” *Journal of Power Sources*, vol. 250, pp. 323–332, 2009.
- [62] Z. A. L. X. L. S.-F. C. G. C. Xu Yidan, Hu Minghui, “State of charge estimation for lithium-ion batteries based on adaptive dual kalman filter,” *Journal of Power Sources*, vol. 77, pp. 1255–1272, 2020.

DEPARTMENT OF ELECTRICAL ENGINEERING

CHALMERS UNIVERSITY OF TECHNOLOGY

Gothenburg, Sweden

www.chalmers.se



CHALMERS
UNIVERSITY OF TECHNOLOGY